# Properties of multi-particle Green and vertex functions within Keldysh formalism

**Severin G Jakobs, Mikhail Pletyukhov and Herbert Schoeller**

Institut für Theoretische Physik A, RWTH Aachen University, D-52056 Aachen, Germany
JARA – Fundamentals of Future Information Technology, Aachen and Jülich, Germany

E-mail: sjakobs@physik.rwth-aachen.de

**Abstract.** The increasing interest in nonequilibrium effects in condensed matter theory motivates the adaption of diverse equilibrium techniques to Keldysh formalism. For methods based on multi-particle Green or vertex functions this involves a detailed knowledge of the real-time properties of those functions. In this review, we derive general properties of fermionic and bosonic multi-particle Green and vertex functions for a stationary state described within Keldysh formalism. Special emphasis is put on the analytic properties associated with causality and on a detailed discussion of the Kubo-Martin-Schwinger conditions which characterize thermal equilibrium. Finally we describe how diagrammatic approximations and approximations within the functional renormalization group approach respect these properties.

PACS numbers: 05.70.Ln, 11.30.Er

## 1. Introduction

Multi-particle Green and vertex functions are an important tool for the theoretical analysis of interacting quantum systems in condensed matter physics. $n$-particle Green functions contain the relevant information to compute $n$-particle properties of the system [1]. Moreover, determining multi-particle functions may be an auxiliary step on the way to find the single-particle Green function (or an approximation to it) and single-particle properties. For example, the functional renormalization group (fRG) approach [2] leads to a system of flow equations which couples all $n$-particle functions with $n \geq 1$ in an infinite hierarchy. Depending on the particular fRG scheme, these $n$-particle functions may be Green or irreducible vertex functions. Another example is given by diagrammatic resummation techniques based on the Bethe-Salpeter equations, such as fluctuation exchange [3] or parquet-equations [4, 5]. For these approaches the preliminary task is to determine the irreducible two-particle vertex function, from which in turn the single-particle self-energy can be deduced.

The methods mentioned above are typically used within zero-temperature or equilibrium formalism. Calculations in equilibrium formalism are based on imaginary frequencies and require an analytic continuation to real frequencies in order to determine many physical observables of interest. At finite temperature, such analytic continuation is numerically quite nontrivial even for a single frequency (see e.g. [6] and references therein). Therefore a formulation of the problem within the real-time (real-frequency) Keldysh formalism [7, 8, 9] may be advantageous. Beyond that, Keldysh formalism allows for the description of nonequilibrium situations such as stationary state transport at finite bias voltage.

A central ingredient of Keldysh formalism is a time contour consisting of two branches, one of them describing evolution forward and the other backward in time. As a consequence of the existence of these two branches, the $n$-particle Green function is a tensor in 2-dimensional space of rank $2n$, having $2^{2n}$ components, each being a function of $2n$ state indices and $2n$ frequencies [or $(2n-1)$ frequencies in the case of time translational invariance]. The resulting additional complexity of the formalism is however reduced due to the fact that the components are not independent from each other but obey certain relations connecting them. In this review, we give a comprehensive and self-contained presentation of fundamental relations for the multi-particle Green and vertex functions within Keldysh formalism: the behaviour under exchange of particles and under complex conjugation, properties connected to causality and the Kubo-Martin-Schwinger (KMS) conditions characterizing thermal equilibrium. The special single-particle versions of these relations are commonly known, e.g. the fact that retarded and advanced single-particle Green function are adjoint to each other, and the fluctuation dissipation theorem in thermal equilibrium. However, also the general multi-particle versions are required to adapt the above-mentioned methods to Keldysh formalism, for instance for real time implementations of the fRG, which have been initiated in [10, 11].

Some of the properties in question have been analysed in [12, 13] for multi-point Green functions based on real bosonic fields. The adaption of their results to condensed matter problems is far from being obvious due to two major complications. Firstly, condensed matter problems usually involve complex bosonic or Grassmann fermionic operators instead of real bosonic ones. This makes necessary a separate book-keeping of incoming and of outgoing indices (corresponding to annihilation and creation operators) instead of just one type of indices as for real bosons. Additionally, due to the commutation relations of complex bosonic or Grassmann fermionic operators, the initial order of a time-ordered operator product is relevant for the result, as opposed to real bosons. Furthermore, the time reversal properties of the field operators which are important for the analysis of the KMS conditions differ from those of real bosonic field operators. The second source of complication is due to the

fact that condensed matter problems usually involve external potentials which lift diverse symmetries of the system. Reference [13] implicitly assumes translational invariance in space and time and invariance under the product of time reversal and parity. These prerequisites, which considerably simplify the investigation of the KMS conditions, are not given in typical condensed matter problems. Despite these fundamental differences some of the concepts developed in references [12, 13] can be fruitfully adapted to our analysis.

In section 2, we start by a short description of the physical situation under consideration. The set-up of an interacting quantum system coupled to a number of noninteracting reservoirs represents a typical stationary state configuration described in Keldysh formalism.

We continue by specifying precisely the definitions of the Green and vertex functions in question in section 3. Here it is necessary to take care of the details (like prefactor conventions) since the exact form of the relations to be discussed depends on them.

In sections 4.1 and 4.2 we derive useful relations connected to the permutation of particles and to complex conjugation. Section 4.3 focuses on a theorem of causality [12] which we cast in concise form. We show that this theorem has direct consequences for the analytic properties of the Green and vertex functions in Fourier space and identify components which are analytic in one half plane of each of their $(2n-1)$ independent frequency arguments. Remarkably, our derivation does not use the Lehmann representation. This fact is highly advantageous due to the unwieldy form the latter acquires in the multiparticle case.

Section 5 is devoted to the special situation of thermal equilibrium. The fact that the density matrix then corresponds to a time evolution in imaginary time is at the root of the KMS conditions [14, 15]. In section 5.1, we describe how to concisely formulate the multi-particle KMS conditions exploiting the so-called tilde Green function which is defined on the analogy of [13] by means of a non-standard ordering of operators on the Keldysh contour. However, in order to extract useful information from the KMS conditions, the tilde Green function has to be eliminated in favour of the standard Green function. In sections 5.3 and 5.4 we find that time reversal can be used for this purpose, an observation similar to the one of [12] for multi-point Green functions based on real bosons. In section 5.5 we characterize an important class of systems (including e.g. the Anderson impurity model [16]) with specific time reversal properties. For this class, we formulate a multi-particle FDT in section 5.6.

Finally we study under which conditions approximations to the Green or vertex functions conserve the before-mentioned properties (section 6). These conditions turn out to be quite handy for the large class of diagrammatic approximations. For approximations within the fRG framework, the choice of the flow parameter is found to be crucial for the conservation of causal features and of the KMS conditions.

## 2. The system under consideration

The physical setup underlying our considerations is a finite interacting quantum system of a single kind of either bosonic or fermionic particles which is coupled to $M$ noninteracting reservoirs, $M \geq 1$. Let $\{q\} = \{s\} \cup \{r_1\} \cup \ldots \cup \{r_M\}$ be a basis of single-particle states which are either localized in the system (states $s$) or in one of the reservoirs (states $r_k$, $k = 1, \ldots, M$). We use the index $q$ to refer to any of those states. The total Hamiltonian under consideration is given by

$$H = H_{\mathrm{sys}} + \sum_{k=1}^{M} H_{\mathrm{res}}^{(k)} + \sum_{k=1}^{M} H_{\mathrm{coup}}^{(k)}, \tag{1}$$

with

$$H_{\rm sys} = \sum_{s,s'} h_{s'|s} a^\dagger_{s'} a_s + \frac{1}{4} \sum_{\substack{s_1,s_1' \\ s_2,s_2'}} \overline{v}_{s_1's_2'|s_1s_2} a^\dagger_{s_1'} a^\dagger_{s_2'} a_{s_2} a_{s_1}, \tag{2}$$

$$H^{(k)}_{\rm res} = \sum_{r_k,r_k'} h_{r_k'|r_k} a^\dagger_{r_k'} a_{r_k}, \tag{3}$$

$$H^{(k)}_{\rm coup} = \sum_{s,r_k} h_{s|r_k} a^\dagger_s a_{r_k} + \text{H.c.} \tag{4}$$

in standard notation of second quantitation. Here

$$h_{q'|q} = \langle q'|h|q\rangle = h^*_{q|q'} \tag{5}$$

are the matrix elements of the single-particle Hamiltonian and

$$\overline{v}_{s_1's_2'|s_1s_2} = \langle s_1's_2'|v|s_1s_2\rangle + \zeta \langle s_1's_2'|v|s_2s_1\rangle \tag{6}$$

denote the (anti-)symmetrized matrix elements of the two-particle interaction, with

$$\zeta = \begin{cases} +1 & \text{for bosons,} \\ -1 & \text{for fermions.} \end{cases} \tag{7}$$

At some initial time $t_0$ the whole configuration is assumed to be described by the density matrix

$$\rho(t_0) = \rho_{\rm sys} \otimes \rho^{(1)}_{\rm res} \otimes \ldots \otimes \rho^{(M)}_{\rm res}, \tag{8}$$

where

$$\rho^{(k)}_{\rm res} = \frac{\mathrm{e}^{-\beta_k(H_k - \mu_k N_k)}}{\mathrm{Tr}\,\mathrm{e}^{-\beta_k(H_k-\mu_k N_k)}}, \qquad k = 1,\ldots,M, \tag{9}$$

is the grand-canonical distribution of reservoir $k$ with temperature $T_k = 1/\beta_k$ and chemical potential $\mu_k$. Keldysh formalism allows us to compute properties described by the density matrix $\rho(t)$, $t > t_0$, which evolves unitarily from $\rho(t_0)$ under the full Hamiltonian $H$ given in (1) [7, 8, 9].

In the limit of an infinite reservoir size $L$ and an infinite transient time $t - t_0$ such that $L/u \gg -t_0 \to \infty$ (with $u$ being the particle velocity in the reservoir), expectation values under $\rho(t)$ become stationary and do not depend on the initial density matrix $\rho_{\rm sys}$ of the finite interacting region. We will restrict our considerations to this stationary situation.

A particular stationary situation is a global equilibrium which occurs if all $T_k$ and $\mu_k$ are equal. We specialism to the equilibrium case in section 5. The results found there are also applicable to interacting bulk systems (that is large systems with the Hamiltonian (2)) in thermal equilibrium.

## 3. Definition of the Green and vertex functions

The time- or frequency-dependent $n$-particle Green function is defined by

$$G^{j|j'}_{q|q'}(t|t') = (-\mathrm{i})^n \left\langle T_{\rm c}\, a^{(j_1)}_{q_1}(t_1)\ldots a^{(j_n)}_{q_n}(t_n) a^{(j_n')\dagger}_{q_n'}(t_n')\ldots a^{(j_1')\dagger}_{q_1'}(t_1')\right\rangle, \tag{10}$$

$$G^{j|j'}_{q|q'}(\omega|\omega') = \int \mathrm{d}t_1\ldots\mathrm{d}t_n'\, \mathrm{e}^{\mathrm{i}(\omega\cdot t - \omega'\cdot t')} G^{j|j'}_{q|q'}(t|t'), \tag{11}$$

where $q = (q_1,\ldots,q_n)$, $t = (t_1,\ldots,t_n)$, $\omega = (\omega_1,\ldots,\omega_n)$ and $j = (j_1,\ldots,j_n)$ are multi-indices denoting state, time, frequency and branch of the time contour, respectively. The annihilation

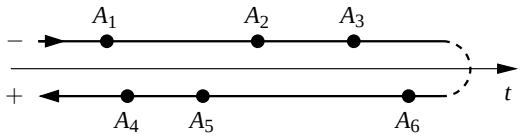


**Figure 1.** The time contour consisting of the $-$- and the $+$-branch with some example operators $A_1,\ldots,A_6$. The time ordering operator $T_c$ will establish the order $A_4A_5A_6A_3A_2A_1$. The operator $\widetilde{T}_c$ used in the definition (41) of the tilde Green function will establish the order $A_6A_5A_4A_1A_2A_3$.

and creation operators $a_{q_k}$ and $a^\dagger_{q_k}$ of a particle in the state $q_k$ obey standard commutation relations

$$[a_{q_1}, a^\dagger_{q_2}]_{-\zeta} = a_{q_1}a^\dagger_{q_2} - \zeta a^\dagger_{q_2}a_{q_1} = \delta_{q_1,q_2}, \tag{12}$$

$$[a_{q_1}, a_{q_2}]_{-\zeta} = [a^\dagger_{q_1}, a^\dagger_{q_2}]_{-\zeta} = 0, \tag{13}$$

and $a^{(j_k)}_{q_k}(t_k)$ denotes an annihilation operator at time $t_k$ in the Heisenberg picture with reference time $t_0$. The operator is situated on the branch $j_k = \mp$ of the time contour [7]. The contour ordering operator $T_c$ in (10) rearranges the sequence of operators in the following way: all operators with $+$-index are placed left of all operators with $-$-index. The block of operators with $+$-index is anti-time ordered internally (which means time arguments of the $+$-operators increase from left to right), whereas the block of operators with $-$-index is time ordered (which means time arguments of the $-$-operators decrease from left to right). By definition of $T_c$ the expression ordered in this way has to be multiplied by a factor $\zeta$, if it represents an odd permutation of the initial order given in (10). The branches of the contour are depicted in figure 1 where also an example for the order established by $T_c$ is given. The expectation value in (10) is defined by

$$\langle A(t)\rangle = \mathrm{Tr}\,\rho(t_0)A(t), \tag{14}$$

with $\rho(t_0)$ being the density operator at time $t_0 \to -\infty$. In (11) we used the shorthand notation $\omega\cdot t = \omega_1 t_1 + \ldots + \omega_n t_n$.

Due to the time translational invariance of the stationary state, the $n$-particle Green function can be expressed as a function of only $(2n-1)$ independent time or frequency arguments. For example $t_1$ and $\omega_1$ can be eliminated by

$$G(t_1,\ldots,t_n|t'_1,\ldots,t'_n) = G(0,t_2-t_1,\ldots,t_n-t_1|t'_1-t_1,\ldots,t'_n-t_1), \tag{15}$$

$$G(\omega_1,\ldots,\omega_n|\omega'_1,\ldots,\omega'_n) = 2\pi\delta(\omega_1+\ldots+\omega_n-\omega'_1-\ldots-\omega'_n) \times G(t_1=0,\omega_2,\ldots,\omega_n|\omega'_1,\ldots,\omega'_n). \tag{16}$$

However, many of the properties discussed in the following are formulated most easily when all time and frequency arguments are treated on equal footing. Therefore we will use the reduced number of frequency arguments only occasionally, e.g. for the study of analytic properties in section 4.3.

Apart from Green functions we will also discuss the properties of one-particle irreducible vertex functions. These vertex functions can be derived from a generating functional called effective action which is the Legendre transform of the generating functional for the connected Green functions. Details on this path-integral approach to the irreducible vertex functions can be found for Matsubara formalism e.g. in [1] and for Keldysh formalism in [10]. Since we do not need any recourse to the generating functionals in the following, we choose an equivalent way to introduce the vertex functions which is based on a diagrammatic expansion.

To set up a standard Hugenholtz diagrammatic technique [1] for a problem with instantaneous two-particle interaction $v$, we define the (anti-)symmetrized interaction vertex

$$\bar{v}^{j_1' j_2'|j_1 j_2}_{q_1' q_2'|q_1 q_2}(t_1', t_2'|t_1, t_2) = \delta(t_1 = t_2 = t_1' = t_2')(-j_1)\delta_{j_1=j_2=j_1'=j_2'}\overline{v}_{q_1' q_2'|q_1 q_2} \tag{17}$$

or, in Fourier space,

$$\bar{v}^{j_1' j_2'|j_1 j_2}_{q_1' q_2'|q_1 q_2}(\omega_1', \omega_2'|\omega_1, \omega_2) = 2\pi\delta(\omega_1 + \omega_2 - \omega_1' - \omega_2')(-j_1)\delta_{j_1=j_2=j_1'=j_2'}\overline{v}_{q_1' q_2'|q_1 q_2}, \tag{18}$$

with $\overline{v}_{q_1' q_2'|q_1 q_2}$ given by (6). Since a single Hugenholtz vertex incorporates both the direct and exchange Feynman vertices, this diagrammatic language is especially concise in formulation. According to Wick's theorem, the $n$-particle Green function can be expanded into a sum of diagrams which consist of lines representing the noninteracting one-particle Green function $G^{(0)}$ and of interaction vertices [17].

For the discussion of the vertex function we will restrict ourselves to the frequency representation. The (anti-)symmetrized irreducible $n$-particle vertex function

$$\gamma^{j'|j}_{q'|q}(\omega'|\omega) = \gamma^{j_1' \ldots j_n'|j_1 \ldots j_n}_{q_1' \ldots q_n'|q_1 \ldots q_n}(\omega_1', \ldots, \omega_n'|\omega_1, \ldots, \omega_n) \tag{19}$$

can be defined diagrammatically as the sum of all one-particle irreducible diagrams with $n$ amputated incoming lines (having state, frequency and contour indices $q, \omega, j$) and $n$ amputated outgoing lines (having indices $q', \omega', j'$). In order to evaluate a given diagram, one determines first the symmetry factor $S$ which is defined as the number of permutations of vertices mapping the diagram onto itself. Then one chooses arbitrarily at each vertex the order in which the attached incoming (outgoing) lines are assigned to the incoming (outgoing) indices of the vertex. This order should be kept fixed during the further evaluation. Let $n_{\mathrm{eq}}$ count the pairs of equivalent lines in the diagram, where two lines are called equivalent if they connect the same vertices and run in the same direction. One can define $n_{\mathrm{loop}}$ to be the number of internal loops made up from internal propagators. (Inside a given vertex $\overline{v}_{1'2'|12}$ we assume that one line continues from 1 to $1'$ and the other continues from 2 to $2'$.) Finally, the incoming line $k$ being connected to the outgoing line $P(k')$ via internal lines and vertices determines a permutation $P$ of $\{1', \ldots, n'\}$. The value of the diagram is then given by

$$\frac{\zeta^{n_{\mathrm{loop}}}\zeta^P}{2^{n_{\mathrm{eq}}}S}\frac{(2\pi)^{2n}}{\mathrm{i}^{n-1}}\left[\prod\frac{\mathrm{i}}{(2\pi)^4}\overline{v}\right]\prod G^{(0)}, \tag{20}$$

where one has to integrate over all internal frequencies and sum over all internal states and contour indices. Due to the (anti-)symmetrization of the vertex in (18), the overall sign of the diagram is actually independent of the chosen assignment of lines to indices at each vertex. An example for the application of the diagram rule is given in figure 2. The Hartree-Fock contribution to the one-particle vertex depicted in figure 2 (d) for instance is evaluated as

$$\zeta(2\pi)^2\frac{i}{(2\pi)^4}\sum_{j_2, j_2'}\sum_{q_2, q_2'}\int \mathrm{d}\omega_2 \mathrm{d}\omega_2' \overline{v}^{j_1' j_2'|j_1 j_2}_{q_1' q_2'|q_1 q_2}(\omega_1' \omega_2'|\omega_1 \omega_2) G^{(0)\, j_2|j_2'}_{\quad q_2|q_2'}(\omega_2|\omega_2'). \tag{21}$$

Given time translational invariance one often works with vertex functions depending on $(2n-1)$ frequencies only, e.g. $\gamma(t_1' = 0, \omega_2' \ldots \omega_n'|\omega_1 \ldots \omega_n)$. The full vertex function (19) is then given by

$$\gamma(\omega_1', \ldots, \omega_n'|\omega_1, \ldots, \omega_n) = 2\pi\delta(\omega_1' + \ldots + \omega_n' - \omega_1 - \ldots - \omega_n) \times\gamma(t_1' = 0, \omega_2', \ldots, \omega_n'|\omega_1, \ldots, \omega_n). \tag{22}$$

The diagrams for $\gamma(t_1' = 0, \omega_2' \ldots \omega_n'|\omega_1 \ldots \omega_n)$ typically consist of single-particle Green functions depending on a single frequency [occurring in the second line of (16)] and

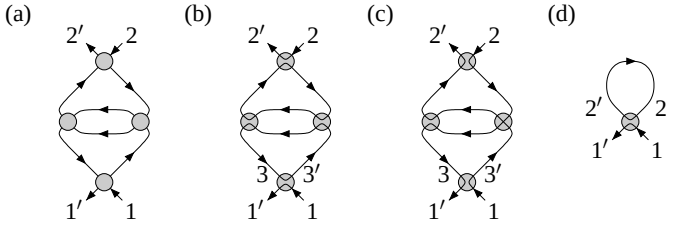


**Figure 2.** Examples for the application of the diagram rules. The lines are free one-particle Green functions, the dots are interaction vertices. The indices represent contour index, state and frequency, e.g. $1 = (j_1, q_1, \omega_1)$. Diagram (a) contributes to the two-particle vertex function. It has one pair of equivalent lines, $n_{\rm eq} = 1$, and no symmetries, $S = 1$. (b) and (c) show two possible, equivalent ways to assign the lines to the indices of the vertices. In (b) the vertex at the bottom e.g. is $\overline{v}_{1'3'|13}$, and $n_{\rm loop} = 2$, $\zeta^P = 1$. In (c) the vertex at the bottom is $\overline{v}_{1'3'|31} = \zeta \overline{v}_{1'3'|13}$, and $n_{\rm loop} = 0$, $\zeta^P = \zeta$. Compared to (b), three of the four vertices acquire a factor $\zeta$; taking into account the prefactor $\zeta^{n_{\rm loop}} \zeta^P$ the possibilities (b) and (c) hence lead to the same value of the diagram. The Hartree-Fock diagram (d) ($n_{\rm eq} = 0$, $S = 1$) contributes to the one-particle vertex, that is the self-energy. The figure shows the evaluation with vertex $\overline{v}_{1'2'|12}$ and $n_{\rm loop} = 1$.

of frequency independent vertices [the part $(-j_1)\delta_{j_1=j_2=j_1'=j_2'} \overline{v}_{q_1' q_2'|q_1 q_2}$ of (18)]. When evaluating such diagrams, the factor $(2\pi)^{2n}$ in (20) has to be replaced by $(2\pi)^{n-1}$ and $\mathrm{i}/(2\pi)^4$ by $\mathrm{i}/(2\pi)$. For the Hartree-Fock diagram in figure 2 (d) e.g. this yields

$$\zeta \frac{i}{2\pi} \sum_{j_2, j_2'} \sum_{q_2, q_2'} \int \mathrm{d}\omega_2 \, \overline{v}^{j_1' j_2'|j_1 j_2}_{q_1' q_2'|q_1 q_2} G^{(0)\, j_2|j_2'}_{\quad\ q_2|q_2'}(\omega_2). \tag{23}$$

Equation (20) defines the prefactor of the vertex functions in such a way, that they can be used themselves as vertices in diagrams with the identical prefactor rules being applicable as for the bare $n$-particle interaction vertices. The self-energy is equal to the one-particle vertex, $\Sigma \equiv \gamma_{n=1}$.

In the one-particle case it is common to call the components of the Green and vertex function chronological, lesser, greater and antichronological,

$$G^{\rm c} = G^{-|-}, \qquad G^{<} = G^{-|+}, \qquad G^{>} = G^{+|-}, \qquad G^{\tilde{\rm c}} = G^{+|+}, \tag{24}$$

$$\Sigma^{\rm c} = \gamma^{-|-}, \qquad \Sigma^{<} = \gamma^{-|+}, \qquad \Sigma^{>} = \gamma^{+|-}, \qquad \Sigma^{\tilde{\rm c}} = \gamma^{+|+}, \tag{25}$$

respectively.

Apart from the contour basis with indices $j_k = \mp$ we will use the Keldysh basis [18] with indices $\alpha_k = 1, 2$ whose components have a direct physical interpretation in terms of response and correlations [19]. The transformation to the Keldysh basis is defined by a change of operators,

$$a^{(1)} = \frac{a^{(-)} - a^{(+)}}{\sqrt{2}}, \qquad a^{(2)} = \frac{a^{(-)} + a^{(+)}}{\sqrt{2}}. \tag{26}$$

The Green and vertex functions change according to the tensor transformation laws,

$$G^{\alpha|\alpha'} = (D^{-1})^{\alpha|j} \, G^{j|j'} \, D^{j'|\alpha'}, \tag{27}$$

$$\gamma^{\alpha'|\alpha} = (D^{-1})^{\alpha'|j'} \, \gamma^{j'|j} \, D^{j|\alpha}, \tag{28}$$

where an implicit summation over all internal indices is assumed, and

$$D^{j|\alpha} = \prod_{k=1}^{n} D^{j_k|\alpha_k}, \tag{29}$$

$$D^{-|1} = D^{\mp|2} = \frac{1}{\sqrt{2}}, \quad D^{+|1} = -\frac{1}{\sqrt{2}}, \tag{30}$$

$$(D^{-1})^{1|-} = (D^{-1})^{2|\mp} = \frac{1}{\sqrt{2}}, \quad (D^{-1})^{1|+} = -\frac{1}{\sqrt{2}}. \tag{31}$$

In the particular case of one-particle functions, we have

$$G^{1|1} = 0, \qquad G^{1|2} = G^{\mathrm{Av}}, \qquad G^{2|1} = G^{\mathrm{Ret}}, \qquad G^{2|2} = G^{\mathrm{K}}, \tag{32}$$

$$\gamma^{1|1} = \Sigma^{\mathrm{K}}, \qquad \gamma^{1|2} = \Sigma^{\mathrm{Ret}}, \qquad \gamma^{2|1} = \Sigma^{\mathrm{Av}}, \qquad \gamma^{2|2} = 0, \tag{33}$$

where the retarded, advanced and Keldysh component of the Green function and the self-energy are given by

$$G^{\mathrm{Ret}}_{q|q'}(t|t') = -\mathrm{i}\Theta(t-t')\left\langle \left[a_q(t), a^\dagger_{q'}(t')\right]_{-\zeta}\right\rangle, \tag{34}$$

$$G^{\mathrm{Av}}_{q|q'}(t|t') = \mathrm{i}\Theta(t'-t)\left\langle \left[a_q(t), a^\dagger_{q'}(t')\right]_{-\zeta}\right\rangle, \tag{35}$$

$$G^{\mathrm{K}}_{q|q'}(t|t') = -\mathrm{i}\left\langle \left[a_q(t), a^\dagger_{q'}(t')\right]_{\zeta}\right\rangle, \tag{36}$$

and

$$G^{\mathrm{Ret}} = G^{(0)\mathrm{Ret}} + G^{(0)\mathrm{Ret}} \circ \Sigma^{\mathrm{Ret}} \circ G^{\mathrm{Ret}}, \tag{37}$$

$$G^{\mathrm{Av}} = G^{(0)\mathrm{Av}} + G^{(0)\mathrm{Av}} \circ \Sigma^{\mathrm{Av}} \circ G^{\mathrm{Av}}, \tag{38}$$

$$G^{\mathrm{K}} = G^{\mathrm{Ret}} \circ \Sigma^{\mathrm{K}} \circ G^{\mathrm{Av}}. \tag{39}$$

Here we use "$\circ$" as a shorthand for summation over internal states and integration over internal times,

$$(A \circ B)_{q|q'}(t|t') = \sum_r \int \mathrm{d}s\, A_{q|r}(t|s) B_{r|q'}(s|t'). \tag{40}$$

When discussing the KMS condition in section 5.1 we will need yet another type of Green function, the so-called tilde Green function which we define on the analogy of [13]. It is given by

$$\widetilde{G}^{j|j'}_{q|q'}(t|t') = (-\mathrm{i})^n \left\langle \widetilde{T}_{\mathrm{c}}\, a^{(j_1)}_{q_1}(t_1) \ldots a^{(j_n)}_{q_n}(t_n) a^{(j'_n)\dagger}_{q'_n}(t'_n) \ldots a^{(j'_1)\dagger}_{q'_1}(t'_1)\right\rangle, \tag{41}$$

$$\widetilde{G}^{j|j'}_{q|q'}(\omega|\omega') = \int \mathrm{d}t_1 \ldots \mathrm{d}t'_n\, \mathrm{e}^{\mathrm{i}(\omega\cdot t - \omega'\cdot t')} \widetilde{G}^{j|j'}_{q|q'}(t|t'), \tag{42}$$

which differs from (10) and (11) only by the other ordering operator $\widetilde{T}_{\mathrm{c}}$. Like $T_{\mathrm{c}}$, $\widetilde{T}_{\mathrm{c}}$ places all operators with $+$-index left of all operators with $-$-index. However, under $\widetilde{T}_{\mathrm{c}}$ the block of operators with $+$-index is time ordered internally, whereas the block of operators with $-$-index is anti-time ordered. Again, if the final order is an odd permutation of the initial one it has to be multiplied by a factor $\zeta$. An example for the order established by $\widetilde{T}_{\mathrm{c}}$ is given in figure 1.

For the one-particle case it is straightforward to check the identity

$$\widetilde{G}^{j|j'}_{q|q'}(t|t') = G^{\bar{j}'|\bar{j}}_{q|q'}(t|t'), \quad n = 1, \tag{43}$$

where a bar over a contour index indicates a swap of the branch, $\bar{j} = -j$ for $j = \mp$. However, in the general multi-particle case there is no direct possibility to express the tilde Green function through an ordinary Green function since the orders established by $T_{\mathrm{c}}$ and $\widetilde{T}_{\mathrm{c}}$ are inherently different; we will need to make use of time reversal to connect both quantities, see section 5.3. A direct consequence of having a special relation for $n = 1$ is the particular structure of the single-particle FDT, see section 5.2.

## 4. General properties of the Green and vertex functions

This section is devoted to properties of the Green and vertex functions which are valid in a general steady state, whereas section 5 focuses on the particular case of thermal equilibrium. We will derive the properties of the Green functions starting out from (10) and (11). Once we know a certain relation for the Green function we can study its implications for the amputated irreducible diagrams, the values of which are given by (20). This will allow us to infer a corresponding relation for the irreducible vertex functions.

### *4.1. Permutation of particles*

Let $P$ be a permutation of $(1,\ldots,n)$ and for any multi-index $b=(b_1,\ldots,b_n)$ define $Pb:=(b_{P(1)},\ldots,b_{P(n)})$. The prefactors $\zeta$ due to time ordering in (10) and due to permutations in (20) entail

$$G^{Pj|j'}_{Pq|q'}(Pt|t') = G^{j|Pj'}_{q|Pq'}(t|Pt') = \zeta^P G^{j|j'}_{q|q'}(t|t'), \tag{44}$$

$$G^{Pj|j'}_{Pq|q'}(P\omega|\omega') = G^{j|Pj'}_{q|Pq'}(\omega|P\omega') = \zeta^P G^{j|j'}_{q|q'}(\omega|\omega'), \tag{45}$$

$$\gamma^{Pj'|j}_{Pq'|q}(P\omega'|\omega) = \gamma^{j'|Pj}_{q'|Pq}(\omega'|P\omega) = \zeta^P \gamma^{j'|j}_{q'|q}(\omega'|\omega). \tag{46}$$

The identical equations hold after transforming to the Keldysh basis. The contour indices $j$ are merely to be replaced by Keldysh indices $\alpha$.

### *4.2. Complex conjugation*

Conjugating (10) interchanges creation and annihilation operators and reverses the order of operators. The reversed order is identical to the order obtained by $T_c$ when each contour index $j_k$ is swapped to its opposite value $-j_k$. Therefore, we find

$$G^{j|j'}_{q|q'}(t|t')^* = (-1)^n G^{\bar{j}'|\bar{j}}_{q'|q}(t'|t) \tag{47}$$

with $\bar{j}=(\bar{j}_1,\ldots\bar{j}_n)$ and $\bar{j}_k=-j_k$. Note that the parity of the permutation needed to establish the order according to $T_c$ is identical for $G^{j|j'}_{q|q'}(t|t')$ and $G^{\bar{j}'|\bar{j}}_{q'|q}(t'|t)$. Hence no additional sign prefactors are required in (47). Fourier transformation leads to

$$G^{j|j'}_{q|q'}(\omega|\omega')^* = (-1)^n G^{\bar{j}'|\bar{j}}_{q'|q}(\omega'|\omega). \tag{48}$$

In order to derive the corresponding identity for the vertex function we discuss how to conjugate the individual diagrams which the vertex function is composed of and whose values are given by (20). The noninteracting single-particle Green functions entering the expression (20) can be conjugated according to (48). The conjugation rule for the bare two-particle interaction vertices in expression (20) is inferred from their definition (18) to be

$$\bar{v}^{j'|j}_{q'|q}(\omega'|\omega)^* = \bar{v}^{j'|j}_{q|q'}(\omega'|\omega) = \bar{v}^{j|j'}_{q|q'}(\omega|\omega') = -\bar{v}^{\bar{j}|\bar{j}'}_{q|q'}(\omega|\omega'), \tag{49}$$

where we make use of $\langle q_1'q_2'|v|q_2q_1\rangle = \langle q_2'q_1'|v|q_1q_2\rangle$ in the first step. Applying (48) and (49) to the conjugate of (20) we find that complex conjugation maps one-to-one the diagrams contributing to $\gamma^{j'|j}_{q'|q}(\omega'|\omega)$ onto those of $\gamma^{\bar{j}|\bar{j}'}_{q|q'}(\omega|\omega')$. The precise relationship can be deduced from the fact that an amputated $n$-particle diagram comprising $m$ two-particle vertices contains $(2m-n)$ free propagators, and is found to be

$$\gamma^{j'|j}_{q'|q}(\omega'|\omega)^* = -\gamma^{\bar{j}|\bar{j}'}_{q|q'}(\omega|\omega'). \tag{50}$$

When transforming to the Keldysh basis via (27) and (28) we use that $D$ is real and fulfils the relation

$$D^{j|\alpha} = (-1)^{\sum_k \alpha_k} (D^{-1})^{\alpha|\bar{j}}, \tag{51}$$

which follows from (29) – (31). We find

$$G^{\alpha|\alpha'}_{q|q'}(\omega|\omega')^* = (-1)^{n+\sum_k(\alpha_k+\alpha'_k)} G^{\alpha'|\alpha}_{q'|q}(\omega'|\omega), \tag{52}$$

$$\gamma^{\alpha'|\alpha}_{q'|q}(\omega'|\omega)^* = (-1)^{1+\sum_k(\alpha_k+\alpha'_k)} \gamma^{\alpha|\alpha'}_{q|q'}(\omega|\omega'). \tag{53}$$

For the one-particle functions, equations (52) and (53) yield the well-known relations

$$G^{\mathrm{Ret}}_{q|q'}(\omega|\omega') = G^{\mathrm{Av}}_{q'|q}(\omega'|\omega)^*, \tag{54}$$

$$G^{\mathrm{K}}_{q|q'}(\omega|\omega') = -G^{\mathrm{K}}_{q'|q}(\omega'|\omega)^*, \tag{55}$$

$$\Sigma^{\mathrm{Ret}}_{q|q'}(\omega|\omega') = \Sigma^{\mathrm{Av}}_{q'|q}(\omega'|\omega)^*, \tag{56}$$

$$\Sigma^{\mathrm{K}}_{q|q'}(\omega|\omega') = -\Sigma^{\mathrm{K}}_{q'|q}(\omega'|\omega)^*. \tag{57}$$

### *4.3. Causality and analyticity*

Consider the Green function $G^{j|j'}(t|t')$ with fixed sets of times $t = (t_1,\ldots,t_n)$, $t' = (t'_1,\ldots t'_n)$, where $t_1$ happens to be the greatest time argument, $t_1 > t_2,\ldots,t'_n$. In this case the order of operators established by $T_{\mathrm{c}}$ is independent of the contour index $j_1$: given $j_1 = -$, $a^{j_1}(t_1)$ is sorted to the leftmost position of all operators with $-$-index; given $j_1 = +$, $a^{j_1}(t_1)$ is sorted to the rightmost position of all operators with $+$-index which is exactly the same place in the total expression as for $j_1 = -$. As a consequence

$$G^{-,j_2\cdots j_n|j'}(t|t') = G^{+,j_2\cdots j_n|j'}(t|t'), \qquad \text{if} \quad t_1 > t_2,\ldots,t'_n. \tag{58}$$

This property is at the heart of a theorem of causality which emerges after transforming (58) to the Keldysh basis. Let us first transform only the contour index $j_1$ to the Keldysh basis:

$$\begin{aligned} G^{\alpha_1,j_2\cdots j_n|j'}(t|t') &= (D^{-1})^{\alpha_1|-} G^{-,j_2\cdots j_n|j'}(t|t') + (D^{-1})^{\alpha_1|+} G^{+,j_2\cdots j_n|j'}(t|t') \\ &= \left[(D^{-1})^{\alpha_1|-} + (D^{-1})^{\alpha_1|+}\right] G^{-,j_2\cdots j_n|j'}(t|t'), \qquad \text{if} \quad t_1 > t_2,\ldots,t'_n. \end{aligned} \tag{59}$$

For $\alpha_1 = 1$ we can use

$$(D^{-1})^{1|-} = \frac{1}{\sqrt{2}} = -(D^{-1})^{1|+} \tag{60}$$

to see that (59) vanishes. After transforming the remaining contour indices to the Keldysh basis, we find

$$G^{1,\alpha_2\cdots\alpha_n|\alpha'}(t|t') = 0, \qquad \text{if} \quad t_1 > t_2 \ldots t'_n. \tag{61}$$

The same line of argument holds if any other time from $t_1,\ldots,t'_n$ is the maximum time. [If the maximum time is one of $t'_1,\ldots,t'_n$ we use $D^{-|1} = -D^{+|1}$ instead of (60).] This leads us to the following *theorem of causality* [12]: the Green function $G^{\alpha|\alpha'}(t|t')$ vanishes if the Keldysh index associated with the strictly greatest time argument equals 1. (The theorem does not apply when multiple time arguments have simultaneously the maximum value. However, this particular configuration has a vanishing measure in the $2n$-dimensional time space.)

A special case is given when all Keldysh indices equal 1,

$$G^{1\ldots1|1\ldots1} \equiv 0. \tag{62}$$

If only one of all Keldysh indices equals 2 the corresponding time argument has to be the greatest one for a nonvanishing Green function. This has a direct impact on the analytic properties of the Green function in frequency space as we will show now.

Consider the Green function $G^{21\ldots1|1\ldots1}$ with all Keldysh indices being 1 except for $\alpha_1 = 2$. Due to the theorem of causality $G^{21\ldots1|1\ldots1}(t_1\ldots t_n|t_1'\ldots t_n')$ is nonvanishing only for $t_1 > t_2,\ldots,t_n'$. For the Fourier transform (16) this means that the integration range of $t_2,\ldots t_n'$ is bounded from above by $t_1$,

$$G^{21\ldots1|1\ldots1}(t_1=0,\omega_2,\ldots,\omega_n|\omega') = \int_{-\infty}^{0} \mathrm{d}t_2\ldots\mathrm{d}t_n' \, \mathrm{e}^{\mathrm{i}(\omega_2 t_2+\ldots+\omega_n t_n-\omega'\cdot t')} \times G^{21\ldots1|1\ldots1}(t_1=0,t_2,\ldots,t_n|t'). \quad (63)$$

$G^{21\ldots1|1\ldots1}(t|t')$ decays if any of $|t_k - t_1|, |t_k' - t_1|$ goes to infinity [which makes the integral in (63) converge]. Due to the upper boundary for the integration range of $t_2,\ldots,t_n$, only the decay for $t_2,\ldots,t_n \to -\infty$ will create poles (branch-cuts) in the upper half plane (uhp) of $\omega_2,\ldots\omega_n$. However, the Green function will be analytic in the lower half plane (lhp) of these frequencies since nonanalytic features in the lhp corresponding to decays in the limit $t_2,\ldots,t_n \to +\infty$ do not appear due to the restriction $t_2,\ldots,t_n < t_1$. In the same way, $G^{21\ldots1|1\ldots1}(t_1=0,\omega_2\ldots\omega_n|\omega_1'\ldots\omega_n')$ can be proven to be analytic in the uhp of $\omega_1'\ldots\omega_n'$. The differing half planes of analyticity for the $\omega_k$ and $\omega_k'$ stem from the different sign conventions for $\omega$ and $\omega'$ in the exponential $\mathrm{e}^{\mathrm{i}(\omega\cdot t-\omega'\cdot t')}$ of the Fourier transform.

The same line of argument holds if any other Keldysh index from $\alpha_1,\ldots\alpha_n'$ equals 2, the rest being 1. Hence we can formulate a *theorem of analyticity*: The Green functions

$$\begin{aligned}
&G^{21\ldots1|1\ldots1}(t_1,\omega_2,\ldots,\omega_n|\omega_1',\ldots,\omega_n'),\\
&G^{121\ldots1|1\ldots1}(\omega_1,t_2,\omega_3,\ldots,\omega_n|\omega_1',\ldots,\omega_n'),\\
&\ldots,\\
&G^{1\ldots1|1\ldots121}(\omega_1,\ldots,\omega_n|\omega_1',\ldots,\omega_{n-2}',t_{n-1}',\omega_n'),\\
&G^{1\ldots1|1\ldots12}(\omega_1,\ldots,\omega_n|\omega_1',\ldots,\omega_{n-1}',t_n')
\end{aligned} \quad (64)$$

are analytic in the lhp of the frequencies $\omega_1,\ldots,\omega_n$ and analytic in the uhp of the frequencies $\omega_1',\ldots,\omega_n'$. These $2n$ special Green functions describe higher order response functions. Being formulated for bosons in time space, they are correspondingly given by the expectation value of a series of nested commutators [19, 12].

The irreducible vertex functions obey a *theorem of causality* as well: the vertex function $\gamma^{\alpha'|\alpha}(t'|t)$ vanishes if the Keldysh index associated with the strictly greatest time argument equals 2.

The proof of this theorem is based on the structure of the diagrams contributing to $\gamma^{\alpha'|\alpha}(t'|t)$. Consider such a one-particle irreducible diagram $d^{\alpha'|\alpha}(t'|t)$ and suppose e.g. $\alpha_1 = 2$. We show that a nonvanishing contribution to the diagram necessitates that at least one time argument from $t_2,\ldots t_n'$ is greater or equal $t_1$.

The diagram is composed of bare two-particle vertices which are connected by internal propagators. The vertices and propagators contribute to the value of the diagram multiplicatively, as described in (20). Some of the vertices have one or two amputated external lines which correspond to the indices of the diagram. When transformed to the Keldysh basis, the bare two-particle vertex given in (17) acquires the form

$$\bar{v}^{\alpha_1'\alpha_2'|\alpha_1\alpha_2}(t_1',t_2'|t_1,t_2) \sim \begin{cases} \delta(t_1=t_2=t_1'=t_2'), & \text{if } \alpha_1+\alpha_2+\alpha_1'+\alpha_2' \text{ is odd,} \\ 0, & \text{else.} \end{cases} \quad (65)$$

According to this equation all four time arguments of a given vertex are equal. Therefore the vertex carrying $t_1$ as external time argument has its other three time arguments equal to $t_1$ as well. If there is an external one among those three, then $t_1$ is not the strictly greatest external time argument. Let us now suppose that the other three time arguments are internal ones. As $\alpha_1 = 2$, at least one of the vertex' three internal Keldysh indices equals 1, see equation (65). There is an internal one-particle Green function attached to this Keldysh index 1. At its other end this Green function is attached to a Keldysh index 2 (since $G^{1|1} = 0$) and a time $\tau_1 \geq t_1$; this follows from the theorem of causality for the Green functions. Actually all four time arguments of the vertex attached to the back-end of the Green function are equal to $\tau_1 \geq t_1$. If there is an external one among them, then $t_1$ is again not the strictly greatest external time argument. If not, this vertex also has as least one Keldysh index equal to 1. Again there is attached a one-particle Green function leading to a vertex with time $\tau_2 \geq \tau_1 \geq t_1$. We can proceed in this way until we arrive finally at a vertex with time $\tau_m \geq \ldots \geq \tau_1 \geq t_1$ which carries an external time argument. This external time argument $\tau_m \geq t_1$ concludes our proof. (There is the possibility that we never end at a vertex with an external line because we can get trapped in a loop of internal vertices with identical time arguments; this case however is of measure zero and vanishes when integrated over internal time arguments.)

We mention two consequences of the theorem of causality for the vertex function which can be derived in the same way as their counterparts for the Green functions. First we conclude that

$$\gamma^{2\ldots2|2\ldots2} \equiv 0. \tag{66}$$

Second, we get a *theorem of analyticity*, namely that the $2n$ vertex functions

$$\begin{aligned}
&\gamma^{12\ldots2|2\ldots2}(t_1', \omega_2', \ldots, \omega_n'|\omega_1, \ldots, \omega_n),\\
&\gamma^{212\ldots2|2\ldots2}(\omega_1', t_2', \omega_3', \ldots, \omega_n'|\omega_1, \ldots, \omega_n),\\
&\ldots,\\
&\gamma^{2\ldots2|2\ldots212}(\omega_1', \ldots, \omega_n'|\omega_1, \ldots, \omega_{n-2}, t_{n-1}, \omega_n),\\
&\gamma^{2\ldots2|2\ldots21}(\omega_1', \ldots, \omega_n'|\omega_1, \ldots, \omega_{n-1}, t_n)
\end{aligned} \tag{67}$$

are analytic in the lhp of the frequencies $\omega_1', \ldots, \omega_n'$ and analytic in the uhp of the frequencies $\omega_1, \ldots, \omega_n$.

For the special case of one-particle functions, the causality properties reduce to the well-known statements

$$G^{1|1} \equiv 0, \qquad \Sigma^{2|2} \equiv 0, \tag{68}$$

and $G^{\mathrm{Ret}}(\omega') \equiv G^{2|1}(t = 0|\omega')$ is analytic in the uhp of $\omega'$, $G^{\mathrm{Av}}(\omega) \equiv G^{1|2}(\omega|t' = 0)$ is analytic in the lhp of $\omega$, $\Sigma^{\mathrm{Ret}}(\omega) \equiv \Sigma^{1|2}(t' = 0|\omega)$ is analytic in the uhp of $\omega$, $\Sigma^{\mathrm{Av}}(\omega') \equiv \Sigma^{2|1}(\omega'|t = 0)$ is analytic in the lhp of $\omega'$.

## 5. Equilibrium properties of the Green and vertex functions

We now focus on the case that the temperatures $T_k = 1/\beta_k$ and chemical potentials $\mu_k$ which determine the reservoir density matrices $\rho_{\mathrm{res}}^{(k)}$ in (9) are all equal,

$$T_k = T, \qquad \mu_k = \mu, \qquad k = 1, \ldots, M. \tag{69}$$

In the limits of infinite reservoir size and infinite transient time, the system is then described by a global equilibrium distribution:

$$G^{j|j'}_{q|q'}(t|t') = (-\mathrm{i})^n \,\mathrm{Tr}\,\rho(t_0) T_{\mathrm{c}}\, a^{(j_1)}_{q_1}(t_1) \ldots a^{(j_1')\dagger}_{q_1'}(t_1')$$

$$\to (-\mathrm{i})^n \,\mathrm{Tr}\,\rho_H(t=0) T_\mathrm{c}\, a_{q_1}^{(j_1)}(t_1)\ldots a_{q_1'}^{(j_1')\dagger}(t_1') \quad \text{for} \quad L/u \gg -t_0 \to \infty \tag{70}$$

with the static equilibrium density matrix

$$\rho_H(t=0) = \rho_H = \frac{\mathrm{e}^{-\beta(H-\mu N)}}{Z}, \qquad Z = \mathrm{Tr}\,\mathrm{e}^{-\beta(H-\mu N)}. \tag{71}$$

Here $H$ is the total Hamiltonian (1) including the quantum system, reservoirs and coupling, and $N$ is the total particle number, which is conserved, $[H,N]=0$. A proof of (70) for coordinate space Green functions has been given recently in [20] for the particular case of a spin impurity model.

In the present section we imply (70) to hold and can therefore replace the expectation value (14) used in (10) and (41) by

$$\langle A(t)\rangle = \mathrm{Tr}\,\rho_H A(t), \tag{72}$$

where the Heisenberg picture now has the reference time $t=0$.

We just described how a thermal equilibrium situation is generated by the coupling to large equilibrated reservoirs. In this way, equilibrium and the stationary nonequilibrium introduced in section 2 are embedded in a common framework. However, the following discussion holds also for equilibrium interacting bulk systems. The only preconditions are the equations (71) and (72), where $H$ is the total Hamiltonian.

### *5.1. Kubo-Martin-Schwinger conditions*

Any operator $A(t)$ in the Heisenberg picture fulfils

$$A(t-\mathrm{i}\beta) = \mathrm{e}^{\beta H} A(t) \mathrm{e}^{-\beta H} = \rho_H^{-1} \mathrm{e}^{\beta\mu N} A(t) \mathrm{e}^{-\beta\mu N} \rho_H. \tag{73}$$

Using the cyclic property of the trace, we can reshuffle two operators at times $t_A$, $t_B$ in a correlation function,

$$\mathrm{Tr}\,\rho_H A(t_A-\mathrm{i}\beta) B(t_B) = \mathrm{Tr}\,\rho_H B(t_B) \mathrm{e}^{\beta\mu N} A(t_A) \mathrm{e}^{-\beta\mu N}. \tag{74}$$

We are going to apply this relation, also known as Kubo-Martin-Schwinger (KMS) condition [14, 15], to the $n$-particle Green function. Given a set of contour indices $j=(j_1,\ldots,j_n)$ and times $t=(t_1,\ldots,t_n)$ define $t-\mathrm{i}\beta_+(j)$ as the set of times obtained from $t$ by adding $(-\mathrm{i}\beta)$ to every $t_k$ with $j_k=+$. For example, given $n=4$ and $j=(-,+,+,-)$, we have $t-\mathrm{i}\beta_+(j) = (t_1, t_2-\mathrm{i}\beta, t_3-\mathrm{i}\beta, t_4)$. Let us prescribe that $T_\mathrm{c}$ orders operators with complex time arguments according to the real parts of their time arguments. Identifying $A$ in (74) with the block of anti-time ordered operators from the $+$-branch and $B$ with the block of time ordered operators from the $-$-branch, we find

$$G_{q|q'}^{j|j'}\Big(t-\mathrm{i}\beta_+(j)\Big|t'-\mathrm{i}\beta_+(j')\Big) = \zeta^{M^{j|j'}} \mathrm{e}^{\beta\mu m^{j|j'}} \widetilde{G}_{q|q'}^{\bar{j}|\bar{j}'}(t|t') = \zeta^{m^{j|j'}} \mathrm{e}^{\beta\mu m^{j|j'}} \widetilde{G}_{q|q'}^{\bar{j}|\bar{j}'}(t|t') \tag{75}$$

with $\widetilde{G}$ being defined in (41) and $m^{j|j'}$ denoting the excess of creation over annihilation operators on the $+$-branch,

$$m^{j|j'} = \sum_{\substack{k=1,\ldots,n:\\ j_k'=+}} 1 - \sum_{\substack{k=1,\ldots,n:\\ j_k=+}} 1. \tag{76}$$

The factor $\zeta^{M^{j|j'}}$ in (75) is due to the different parity of the permutations which are required to sort

$$a^{(j_1)}(t_1)\ldots a^{(j_n)}(t_n) a^{(j_n')\dagger}(t_n')\ldots a^{(j_1')\dagger}(t_1') \tag{77}$$

according to $T_c$ and to sort

$$a^{(\bar{j}_1)}(t_1)\dots a^{(\bar{j}_n)}(t_n)a^{(\bar{j}_n)\dagger}(t'_n)\dots a^{(\bar{j}'_1)\dagger}(t'_1) \tag{78}$$

according to $\widetilde{T}_c$. This difference can be computed from the number $M^{j|j'}$ of pairwise swaps of adjacent operators needed to exchange the ordered block of operators from the $+$-branch with the ordered block of operators from the $-$-branch,

$$M^{j|j'} = \left[\sum_{k:j'_k=+} 1 + \sum_{k:j_k=+} 1\right]\left[\sum_{k:j'_k=-} 1 + \sum_{k:j_k=-} 1\right]. \tag{79}$$

In (75) we have used that

$$\zeta^{M^{j|j'}} = \zeta^{m^{j|j'}}, \tag{80}$$

which is a consequence of having an even number $2n$ of indices. The rewriting in terms of $m^{j|j'}$ turns out to be more convenient in the following computation.

When transforming (75) to Fourier space, we substitute on the left hand side $t_k - \mathrm{i}\beta \to t_k$, $t'_k - \mathrm{i}\beta \to t'_k$ for all time arguments on the $+$-branch and find

$$\begin{aligned}\mathrm{e}^{\beta\Delta^{j|j'}(\omega|\omega')} \int_{-\infty-\mathrm{i}\beta}^{\infty-\mathrm{i}\beta} \left[\prod_{k:j_k=+} \mathrm{d}t_k\right]\left[\prod_{k:j'_k=+} \mathrm{d}t'_k\right] \\ \times \int_{-\infty}^{\infty} \left[\prod_{k:j_k=-} \mathrm{d}t_k\right]\left[\prod_{k:j'_k=-} \mathrm{d}t'_k\right] \mathrm{e}^{\mathrm{i}(\omega\cdot t - \omega'\cdot t')} G^{j|j'}_{q|q'}(t|t') = \zeta^{m^{j|j'}} \widetilde{G}^{\bar{j}|\bar{j}'}_{q|q'}(\omega|\omega'),\end{aligned} \tag{81}$$

where $\Delta^{j|j'}(\omega|\omega')$ is defined as

$$\Delta^{j|j'}(\omega|\omega') = \sum_{k:j'_k=+} (\omega'_k - \mu) - \sum_{k:j_k=+} (\omega_k - \mu). \tag{82}$$

As next step we shift the path of integration for all time arguments on the $+$-branch by $(+\mathrm{i}\beta)$ on the left hand side of (81) in order to obtain a standard Fourier integral along the real axis.

This simultaneous shift of integration paths actually does not change the value of the integral, as we explain now. In principle the shift of a single time argument will change the value of the integral because $G^{j|j'}(t|t')$ is in general not analytic in any single $t_k$ or $t'_k$; branch-cuts occur due to changed time ordering whenever a creation and annihilation operator of the same state and on the same branch of the contour have coinciding real parts of their time arguments. Suppose e.g. there exist $k_1, k_2 \in \{1,\dots,n\}$ with $j_{k_1} = j'_{k_2} = +$ and $q_{k_1} = q'_{k_2} =: q_0$, that is an annihilation and a creation operator of the same state $q_0$ are both situated on the $+$-branch. For real times $t_{k_1}, t'_{k_2}$ with $t_{k_1}$ approaching $t'_{k_2}$ from above, $t_{k_1} = t'_{k_2} + 0^+$, the contour ordered operator product appearing in (10) will have the structure

$$\dots a^\dagger_{q_0}(t'_{k_2}) a_{q_0}(t'_{k_2})\dots, \tag{83}$$

where the dots represent the other operators and a prefactor $\zeta$ if necessary. But for $t_{k_1}$ approaching $t'_{k_2}$ from below, $t_{k_1} = t'_{k_2} - 0^+$, the structure is

$$\zeta\dots a_{q_0}(t'_{k_2}) a^\dagger_{q_0}(t'_{k_2})\dots = \zeta\dots\left[1 + \zeta a^\dagger_{q_0}(t'_{k_2}) a_{q_0}(t'_{k_2})\right]\dots. \tag{84}$$

Here we use the commutation relation (12). The results (83) and (84) differ by $\zeta$ so that the Green function is discontinuous in $t_{k_1}$. When complex time arguments are allowed for, the discontinuity is stretched to a branch-cut in the complex $t_{k_1}$-plane as sketched in figure 3.

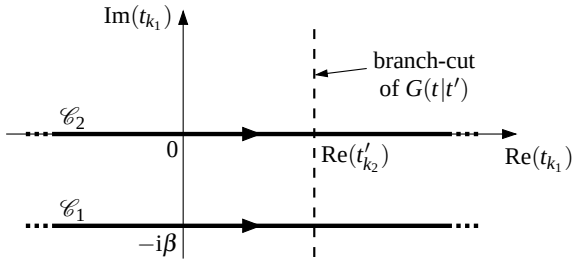


**Figure 3.** If an annihilation operator at time $t_{k_1}$ and a creation operator at time $t'_{k_2}$ are of the same state and are situated on the same branch of the contour, then the Green function $G(t|t')$ has a branch-cut along $\mathrm{Re}(t_{k_1}) = \mathrm{Re}(t'_{k_2})$. In this case the Fourier integrals of $G(t|t')$ over $t_{k_1}$ along the paths $\mathscr{C}_1$ and $\mathscr{C}_2$ are not equal.

However, we do not only shift the integration path of a single time argument but those of all time arguments on the $+$-branch simultaneously. If the dependence on the $n_+$ time arguments on the $+$-branch is expressed through a centre time

$$t_\mathrm{c} = \frac{1}{n_+}\left[\sum_{k:j_k=+} t_k + \sum_{k:j'_k=+} t'_k\right] \tag{85}$$

and $(n_+ - 1)$ relative times, then $G$ is analytic in $t_\mathrm{c}$: a simultaneous change of all times on the $+$-branch by the same value does not affect time ordering. Hence by shifting the integration path of $t_\mathrm{c}$ while keeping all relative times unchanged we do not alter the value of the integral. (Note that the dependence on the relative time arguments might remain nonanalytic.) Therefore equation (81) is equivalent to

$$\mathrm{e}^{\beta\Delta^{j|j'}(\omega|\omega')} G^{j|j'}_{q|q'}(\omega|\omega') = \zeta^{m^{j|j'}}\, \widetilde{G}^{\bar{j}|\bar{j}'}_{q|q'}(\omega|\omega'). \tag{86}$$

### *5.2. Fluctuation dissipation theorem (FDT)*

Equation (86) formulates a relation between $G$ and $\widetilde{G}$. Since $\widetilde{G}$ is a rather artificial object of no direct practical use, it is desirable to eliminate it from (86) in favour of $G$.

In the one-particle case, we can make use of (43) and obtain

$$\mathrm{e}^{\beta\Delta^{j|j'}(\omega|\omega')} G^{j|j'}_{q|q'}(\omega|\omega') = \zeta^{m^{j|j'}}\, G^{j'|j}_{q|q'}(\omega|\omega'), \qquad n = 1. \tag{87}$$

Plugging in $j, j' = \mp$ yields four equations, two of them being tautologies and the other two being equivalent to

$$G^<(\omega) = \zeta \mathrm{e}^{-\beta(\omega-\mu)} G^>(\omega). \tag{88}$$

The Green functions depend only on one frequency argument due to time translational invariance. A transformation to the Keldysh basis yields the well-known FDT, which formulates a relation between the correlation function $G^\mathrm{K}$ and the response functions $G^\mathrm{Ret}$ and $G^\mathrm{Av}$,

$$G^\mathrm{K}(\omega) = \left[1 + \zeta 2 n_\zeta(\omega-\mu)\right]\left[G^\mathrm{Ret}(\omega) - G^\mathrm{Av}(\omega)\right]. \tag{89}$$

Here

$$n_\zeta(\omega) = \frac{1}{\mathrm{e}^{\beta\omega} - \zeta} \tag{90}$$

is the Bose ($\zeta=+1$) or Fermi ($\zeta=-1$) function, and

$$1+\zeta 2n_\zeta(\omega)=\begin{cases}\coth\dfrac{\beta\omega}{2}, & \text{if } \zeta=+1,\\ \tanh\dfrac{\beta\omega}{2}, & \text{if } \zeta=-1.\end{cases} \tag{91}$$

The FDT for the self-energy can be obtained by combining (89) with (37) – (39),

$$\Sigma^{\mathrm{K}}(\omega)=\left[1+\zeta 2n_\zeta(\omega-\mu)\right]\left[\Sigma^{\mathrm{Ret}}(\omega)-\Sigma^{\mathrm{Av}}(\omega)\right]. \tag{92}$$

Transforming this result to the contour basis leads to an analogue of (88),

$$\Sigma^{<}(\omega)=\zeta \mathrm{e}^{-\beta(\omega-\mu)}\Sigma^{>}(\omega). \tag{93}$$

### *5.3. Time reversal*

A direct generalization of (43) to the multi-particle case does not exist. In order to eliminate $\widetilde{G}$ from (86), we should resort to time reversal.

The time reversal operator $\Theta$ is antiunitary, that is $\langle\psi|\Theta\phi\rangle=\langle\phi|\Theta^\dagger\psi\rangle$ and $\Theta\Theta^\dagger=\Theta^\dagger\Theta=1$; for details see e.g. [21]. Its action either on a single-particle state $|q\rangle=|\boldsymbol{x},m\rangle$ in the eigenbasis of position and $s_z$ component of spin or on a state $|\boldsymbol{p},m\rangle$ in the eigenbasis of momentum and $s_z$ is given by

$$\Theta|\boldsymbol{x},m\rangle=\mathrm{e}^{\mathrm{i}\pi m}|\boldsymbol{x},-m\rangle, \tag{94}$$

$$\Theta|\boldsymbol{p},m\rangle=\mathrm{e}^{\mathrm{i}\pi m}|-\boldsymbol{p},-m\rangle. \tag{95}$$

Since the vacuum state $|\mathrm{vac}\rangle$ is time reversal invariant, $\Theta|\mathrm{vac}\rangle=|\mathrm{vac}\rangle$, the transformation of creation and annihilation operators turns out to be

$$\Theta a_q^\dagger\Theta^\dagger=a_{\Theta q}^\dagger,\qquad \Theta a_q\Theta^\dagger=a_{\Theta q}. \tag{96}$$

Explicitly, in the position or momentum basis it reads

$$\Theta a_{\boldsymbol{x},m}^\dagger\Theta^\dagger=\mathrm{e}^{\mathrm{i}\pi m}a_{\boldsymbol{x},-m}^\dagger,\qquad \Theta a_{\boldsymbol{x},m}\Theta^\dagger=\mathrm{e}^{-\mathrm{i}\pi m}a_{\boldsymbol{x},-m}, \tag{97}$$

$$\Theta a_{\boldsymbol{p},m}^\dagger\Theta^\dagger=\mathrm{e}^{\mathrm{i}\pi m}a_{-\boldsymbol{p},-m}^\dagger,\qquad \Theta a_{\boldsymbol{p},m}\Theta^\dagger=\mathrm{e}^{-\mathrm{i}\pi m}a_{-\boldsymbol{p},-m}. \tag{98}$$

We will designate a time reversed state $q$ or operator $A$ by a tilde,

$$\widetilde{q}=\Theta q,\qquad \widetilde{A}=\Theta A\Theta^\dagger. \tag{99}$$

If $\{s\}$ is a complete set of orthonormal many-body states, so is $\{\Theta^\dagger s\}$. (Completeness of $\{\Theta^\dagger s\}$ follows from

$$\langle\psi|\left[\sum_s|\Theta^\dagger s\rangle\langle\Theta^\dagger s|\right]|\phi\rangle=\sum_s\langle s|\Theta\psi\rangle\langle\Theta\phi|s\rangle=\langle\Theta\phi|\Theta\psi\rangle=\langle\psi|\phi\rangle, \tag{100}$$

which holds for any $\psi,\phi$.) Hence, for any operator $A$

$$\mathrm{Tr}A=\sum_s\langle\Theta^\dagger s|A|\Theta^\dagger s\rangle=\sum_s\langle s|\Theta A\Theta^\dagger|s\rangle^*=\left(\mathrm{Tr}\widetilde{A}\right)^*. \tag{101}$$

The time reversed density matrix is given by

$$\widetilde{\rho_H}=\Theta\frac{1}{Z}\mathrm{e}^{-\beta(H-\mu N)}\Theta^\dagger=\frac{1}{Z}\mathrm{e}^{-\beta(\widetilde{H}-\mu N)} \tag{102}$$

with

$$Z=\mathrm{Tr}\mathrm{e}^{-\beta(H-\mu N)}=\left(\mathrm{Tr}\Theta\mathrm{e}^{-\beta(H-\mu N)}\Theta^\dagger\right)^*=\mathrm{Tr}\mathrm{e}^{-\beta(\widetilde{H}-\mu N)}, \tag{103}$$

where we used $N = \widetilde{N}$. Hence

$$\widetilde{\rho_H} = \rho_{\widetilde{H}}. \tag{104}$$

Applying time reversal to an operator in the Heisenberg picture yields

$$\Theta A(t)\Theta^\dagger = \Theta \mathrm{e}^{\mathrm{i}Ht} A \mathrm{e}^{-\mathrm{i}Ht}\Theta^\dagger = \mathrm{e}^{-\mathrm{i}\widetilde{H}t}\widetilde{A}\mathrm{e}^{\mathrm{i}\widetilde{H}t} = \widetilde{A}(-t)\big|_{\widetilde{H}}, \tag{105}$$

where the subscript $|_{\widetilde{H}}$ indicates that time evolution is induced by $\widetilde{H}$ on the right hand side.

From (101), (104) and (105) we conclude for the $n$-particle tilde Green function defined in (41) that

$$\begin{aligned}
\widetilde{G}^{j|j'}_{q|q'}(t|t') &= (-\mathrm{i})^n \operatorname{Tr}\rho_H \widetilde{T}_\mathrm{c}\, a^{(j_1)}_{q_1}(t_1)\ldots a^{(j_1')\dagger}_{q_1'}(t_1') \\
&= (-\mathrm{i})^n \Big[\operatorname{Tr}\Theta\rho_H \widetilde{T}_\mathrm{c}\, a^{(j_1)}_{q_1}(t_1)\ldots a^{(j_1')\dagger}_{q_1'}(t_1')\Theta^\dagger\Big]^* \\
&= (-\mathrm{i})^n \Big[\operatorname{Tr}\rho_{\widetilde{H}} T_\mathrm{c}\, a^{(j_1)}_{\widetilde{q}_1}(-t_1)\big|_{\widetilde{H}}\ldots a^{(j_1')\dagger}_{\widetilde{q}_1'}(-t_1')\big|_{\widetilde{H}}\Big]^* \\
&= (-1)^n \Big[G^{j|j'}_{\widetilde{q}|\widetilde{q}'}(-t|-t')\big|_{\widetilde{H}}\Big]^* \\
&= G^{\bar{j}'|\bar{j}}_{\widetilde{q}'|\widetilde{q}}(-t'|-t)\big|_{\widetilde{H}}.
\end{aligned} \tag{106}$$

Here $\widetilde{q} = (\widetilde{q}_1,\ldots,\widetilde{q}_n)$, and in the last two lines the subscript $|_{\widetilde{H}}$ indicates that both the time evolution and the equilibrium density matrix are determined by $\widetilde{H}$. For the very last step, we use the rule for complex conjugation formulated in (47). In Fourier space, equation (106) reads

$$\widetilde{G}^{j|j'}_{q|q'}(\omega|\omega') = G^{\bar{j}'|\bar{j}}_{\widetilde{q}'|\widetilde{q}}(\omega'|\omega)\big|_{\widetilde{H}}. \tag{107}$$

### *5.4. Combining KMS conditions and time reversal*

Unlike the property (43) of $\widetilde{G}$ which is restricted to the one-particle case, equation (107) holds for any $n$ and provides a general possibility to eliminate $\widetilde{G}$ from (86). Using it we find

$$\mathrm{e}^{\beta\Delta^{j|j'}(\omega|\omega')} G^{j|j'}_{q|q'}(\omega|\omega') = \zeta^{m^{j|j'}} G^{j'|j}_{\widetilde{q}'|\widetilde{q}}(\omega'|\omega)\big|_{\widetilde{H}}, \tag{108}$$

which is a generalization of (87) to arbitrary particle number $n$. We recover formula (87) from (108) by means of

$$G^{j|j'}_{q|q'}(\omega|\omega') = G^{j|j'}_{\widetilde{q}'|\widetilde{q}}(\omega'|\omega)\big|_{\widetilde{H}}\,, \quad n = 1, \tag{109}$$

which follows from combining the Fourier transform of (43) with (107).

If one transforms equation (108) to the Keldysh basis, the result can be considered as a multi-particle FDT since the components of the multi-particle Green functions in the Keldysh basis have a distinct interpretation in terms of response and correlation functions [19]. We perform this transformation in section 5.6, restricting ourselves to a class of physically interesting systems which allow for certain simplifications of the multi-particle FDT.

Before deriving an $n$-particle identity for the vertex function analogous to (108), we note that the bare two-particle interaction vertex given by (18) satisfies

$$\mathrm{e}^{\beta\Delta^{j'|j}(\omega'|\omega)} \bar{v}^{j'|j}_{q'|q}(\omega'|\omega) = \zeta^{m^{j'|j}} \bar{v}^{j|j'}_{\widetilde{q}|\widetilde{q}'}(\omega|\omega')\big|_{\widetilde{H}}. \tag{110}$$

In the case $(j'|j) \notin \{(--|--),(++|++)\}$ this equation is automatically fulfilled because both quantities equal zero. For $(j'|j) \in \{(--|--),(++|++)\}$ equation (110) states

$$\bar{v}^{j'|j}_{q'|q}(\omega'|\omega) = \bar{v}^{j|j'}_{\widetilde{q}|\widetilde{q}'}(\omega|\omega')\big|_{\widetilde{H}} \quad \text{if} \quad j_1' = j_2' = j_1 = j_2 = \mp, \tag{111}$$

which follows from

$$\begin{aligned}\langle q_1' q_2' | v\big(|q_1 q_2\rangle + \zeta |q_2 q_1\rangle\big) &= \big(\langle q_1' q_2'| + \zeta \langle q_2' q_1'|\big)\Theta^\dagger \Theta v \Theta^\dagger \Theta |q_1 q_2\rangle \\ &= \langle \widetilde{q}_1 \widetilde{q}_2 | \widetilde{v}\big(|\widetilde{q}_1' \widetilde{q}_2'\rangle + \zeta |\widetilde{q}_2' \widetilde{q}_1'\rangle\big), \end{aligned} \tag{112}$$

where $\widetilde{v} = \Theta v \Theta^\dagger$.

With help of (110) we can now prove the identity

$$\mathrm{e}^{\beta \Delta^{j'|j}(\omega'|\omega)} \gamma^{j'|j}_{q'|q}(\omega'|\omega) = \zeta^{m^{j'|j}} \gamma^{j|j'}_{\widetilde{q}|\widetilde{q}'}(\omega|\omega')\Big|_{\widetilde{H}} \tag{113}$$

by identifying one by one the diagrams contributing to each side of it. The values of the individual diagrams are given by (20). The prefactors $\mathrm{e}^{\beta \Delta^{j'|j}(\omega'|\omega)}$ and $\zeta^{m^{j'|j}}$ appearing in (113) can be split and distributed among the noninteracting single-particle Green functions and bare two-particle vertices in (20) by making use of the properties

$$\Delta^{j'|j}(\omega'|\omega) = \Delta^{j'|i}(\omega'|\nu) + \Delta^{i|j}(\nu|\omega), \tag{114}$$

$$m^{j'|j} = m^{j'|i} + m^{i|j}, \tag{115}$$

which can be easily generalized to mixed particle numbers and chains of arbitrary length, like e.g.

$$m^{j_1' j_2'|j_1 j_2} = m^{j_1' j_2'|i_1 i_2} + m^{i_1|i_1'} + m^{i_2|i_2'} + m^{i_1' i_2'|j_1 j_2}. \tag{116}$$

According to (108) and (110) the constituents of both sides of (113) can then be readily identified.

### *5.5. Systems with special behaviour under time reversal*

For a further evaluation of (108) and (113), we should establish how the system behaves under time reversal. We restrict the following discussion to the class of systems which satisfy

$$G^{j|j'}_{q|q'}(t|t') = G^{j|j'}_{\widetilde{q}|\widetilde{q}'}(t|t')\big|_{\widetilde{H}} \tag{117}$$

for all indices and time arguments. Note that equation (117) is not only a condition on the Hamiltonian but also on the basis of single-particle states.

We mention some examples which demonstrate the extent of this class of systems. A trivial example for the validity of (117) is given when the Hamiltonian and the single-particle states are time reversal invariant.

As a less trivial example we consider the single impurity Anderson model (SIAM) [16] in a magnetic field $B$. This model consists of an electronic impurity with on-site interaction which is coupled to a conductor. The corresponding Hamiltonian reads

$$\begin{aligned} H_B = &\sum_\sigma (\varepsilon_0 + \sigma B) a_\sigma^\dagger a_\sigma + \sum_\sigma \int d^3p\ \varepsilon_p c^\dagger_{\boldsymbol{p},\sigma} c_{\boldsymbol{p},\sigma} \\ &+ \sum_\sigma \int d^3p\ \big[V_p a_\sigma^\dagger c_{\boldsymbol{p},\sigma} + \text{H.c.}\big] + U a_\uparrow^\dagger a_\uparrow a_\downarrow^\dagger a_\downarrow. \end{aligned} \tag{118}$$

Here $\sigma = \pm\frac{1}{2} = \uparrow, \downarrow$ denote the eigenvalues of the single-particle spin $s_z$, and $c^\dagger, c$ are creators and annihilators of states in the conductor.

As a single-particle basis to be used in (117) we choose the common eigenbasis of position and $s_z$, $|q\rangle = |\boldsymbol{x}, \sigma\rangle$, where the values of $\boldsymbol{x}$ are considered to label the states of both the conductor and the impurity.

In order to verify (117) for this Hamiltonian and this choice of basis, we make use of the unitary transformation $\Omega = \mathrm{e}^{-\mathrm{i}\pi S_x}$ rotating spin space by $\pi$ around the $x$-axis, $S_x$ being the $x$-component of the total spin,

$$\Omega|\boldsymbol{x},\sigma\rangle = -\mathrm{i}|\boldsymbol{x},-\sigma\rangle. \tag{119}$$

Using (98) and the fact that $\varepsilon_p$ and $V_p$ do not depend on the sign of $\boldsymbol{p}$ in (118), we find

$$\widetilde{H_B} = H_{-B} = \Omega H_B \Omega^\dagger. \tag{120}$$

Since a combination of (94) and (119) yields additionally

$$|\widetilde{q}\rangle = \Theta|\boldsymbol{x},\sigma\rangle = \mathrm{e}^{\mathrm{i}\pi(\sigma+\frac{1}{2})}\Omega|\boldsymbol{x},\sigma\rangle = \mathrm{e}^{\mathrm{i}\pi(\sigma+\frac{1}{2})}\Omega|q\rangle \tag{121}$$

we conclude

$$G_{\widetilde{q}|\widetilde{q}'}\big|_{\widetilde{H}} = \mathrm{e}^{\mathrm{i}\pi\sum_k(\sigma_k'-\sigma_k)} G_{\Omega q|\Omega q'}\big|_{\Omega H\Omega^\dagger} = G_{\Omega q|\Omega q'}\big|_{\Omega H\Omega^\dagger} \tag{122}$$

with $\Omega q = (\Omega q_1, \ldots, \Omega q_n)$. In (122) we exploit that the Green function is nonvanishing only for

$$\sum_{k=1}^{N} \sigma_k' = \sum_{k=1}^{N} \sigma_k \tag{123}$$

due to spin conservation. It is straightforward to derive from (10), (71) and (72) that

$$G_{\Omega q|\Omega q'}\big|_{\Omega H\Omega^\dagger} = G_{q|q'}. \tag{124}$$

[Note that (124) holds in general for any unitary operator $\Omega$.] Combining (122) and (124) we conclude that the condition (117) is fulfilled for the impurity model (118) and the single-particle basis $|q\rangle = |\boldsymbol{x},\sigma\rangle$.

On the full analogy it can be shown that (117) is also valid for this impurity model and the single-particle basis $|q\rangle = |\boldsymbol{p},\sigma\rangle$. In (120) – (124), $\Omega$ simply has to be replaced by $\Omega\Pi$, where $\Pi$ is the parity transformation,

$$\Pi|\boldsymbol{p},\sigma\rangle = |-\boldsymbol{p},\sigma\rangle. \tag{125}$$

As an example of a system which does not fulfil (117) we consider the Hamiltonian

$$H_{\boldsymbol{A}} = \int \mathrm{d}^3x\, a_{\boldsymbol{x}}^\dagger \frac{\left[-\mathrm{i}\nabla - e\boldsymbol{A}(\boldsymbol{x})\right]^2}{2m} a_{\boldsymbol{x}} \tag{126}$$

for spinless particles with charge $e$ moving in the field of a vector potential $\boldsymbol{A}(\boldsymbol{x})$. Let us choose the position eigenstates as the single-particle basis. Since

$$\widetilde{H_{\boldsymbol{A}}} = H_{-\boldsymbol{A}}, \tag{127}$$

we conclude that for a generic vector potential

$$G_{\widetilde{\boldsymbol{x}_1}\ldots\widetilde{\boldsymbol{x}_n}|\widetilde{\boldsymbol{x}_1'}\ldots\widetilde{\boldsymbol{x}_n'}}\Big|_{\widetilde{H_{\boldsymbol{A}}}} = G_{\boldsymbol{x}_1\ldots\boldsymbol{x}_n|\boldsymbol{x}_1'\ldots\boldsymbol{x}_n'}\Big|_{H_{-\boldsymbol{A}}} \neq G_{\boldsymbol{x}_1\ldots\boldsymbol{x}_n|\boldsymbol{x}_1'\ldots\boldsymbol{x}_n'}\Big|_{H_{\boldsymbol{A}}}. \tag{128}$$

Obviously, equation (117) does not hold for this choice of Hamiltonian and single-particle basis.

*5.6. Generalized fluctuation dissipation theorem for systems satisfying equation (117)*

When relation (117) holds, equation (108) takes the form

$$\mathrm{e}^{\beta\Delta^{j|j'}(\omega|\omega')}G^{j|j'}_{q|q'}(\omega|\omega') = \zeta^{m^{j|j'}}G^{j'|j}_{q'|q}(\omega'|\omega). \tag{129}$$

Additionally, equation (117) can be expanded in orders of the two-particle interaction. From the first-order term of this expansion of the two-particle Green function, we infer that the bare two-particle interaction vertex complies with

$$\overline{v}^{j'|j}_{q'|q}(\omega'|\omega) = \overline{v}^{j'|j}_{\widetilde{q}'|\widetilde{q}}(\omega'|\omega)\big|_{\widetilde{H}}\,. \tag{130}$$

When combined with (110) it brings about the identity

$$\mathrm{e}^{\beta\Delta^{j'|j}(\omega'|\omega)}\overline{v}^{j'|j}_{q'|q}(\omega'|\omega) = \zeta^{m^{j'|j}}\overline{v}^{j|j'}_{q|q'}(\omega|\omega'). \tag{131}$$

Similarly to the derivation of (113) we deduce from (129) and (131) that

$$\mathrm{e}^{\beta\Delta^{j'|j}(\omega'|\omega)}\gamma^{j'|j}_{q'|q}(\omega'|\omega) = \zeta^{m^{j'|j}}\gamma^{j|j'}_{q|q'}(\omega|\omega'). \tag{132}$$

It is convenient to combine (129) and (132) with (48) and (50), respectively, in order to obtain the equations

$$\mathrm{e}^{\beta\Delta^{j|j'}(\omega|\omega')}G^{j|j'}_{q|q'}(\omega|\omega') = (-1)^n\zeta^{m^{j|j'}}G^{\bar{j}|\bar{j}'}_{q|q'}(\omega|\omega')^*, \tag{133}$$

$$\mathrm{e}^{\beta\Delta^{j'|j}(\omega'|\omega)}\gamma^{j'|j}_{q'|q}(\omega'|\omega) = -\zeta^{m^{j'|j}}\gamma^{\bar{j}'|\bar{j}}_{q'|q}(\omega'|\omega)^*, \tag{134}$$

where state indices and frequency arguments are now identical on both sides.

We are going to transform (133) and (134) to the Keldysh basis in order to achieve a multi-particle FDT. In what follows the state indices are omitted for brevity. According to

$$G^{j|j'} = \sum_{\alpha,\alpha'} D^{j|\alpha}G^{\alpha|\alpha'}(D^{-1})^{\alpha'|j'} \tag{135}$$

every component of $G^{j|j'}$ is expressed as a certain linear combination of components of $G^{\alpha|\alpha'}$. Let us define

$$G^{j|j'}_{\varepsilon} = \sum_{\substack{\alpha,\alpha' \\ (-1)^{\sum_k(\alpha_k+\alpha'_k)}=\varepsilon}} D^{j|\alpha}G^{\alpha|\alpha'}(D^{-1})^{\alpha'|j'} \tag{136}$$

for $\varepsilon = \pm 1$ (cf. [12, 13]). It is obvious that

$$G^{j|j'} = G^{j|j'}_{+} + G^{j|j'}_{-}. \tag{137}$$

Using the relations

$$D^{j|\alpha} = (-1)^{\sum_k\alpha_k}D^{\bar{j}|\alpha}, \tag{138}$$

$$(D^{-1})^{\alpha|j} = (-1)^{\sum_k\alpha_k}(D^{-1})^{\alpha|\bar{j}}, \tag{139}$$

which follow from (29) – (31), we find additionally that

$$G^{\bar{j}|\bar{j}'} = G^{j|j'}_{+} - G^{j|j'}_{-}. \tag{140}$$

Plugging (137) and (140) into (133) and splitting the latter into the real and the imaginary parts we obtain

$$\sinh\tfrac{\beta\Delta^{j|j'}(\omega|\omega')}{2}\ \mathrm{Re}\,G^{j|j'}_{\zeta\varepsilon_n^{j|j'}}(\omega|\omega') = -\cosh\tfrac{\beta\Delta^{j|j'}(\omega|\omega')}{2}\ \mathrm{Re}\,G^{j|j'}_{-\zeta\varepsilon_n^{j|j'}}(\omega|\omega'), \tag{141}$$

$$\cosh\tfrac{\beta\Delta^{j|j'}(\omega|\omega')}{2}\ \mathrm{Im}\,G^{j|j'}_{\zeta\varepsilon_n^{j|j'}}(\omega|\omega') = -\sinh\tfrac{\beta\Delta^{j|j'}(\omega|\omega')}{2}\ \mathrm{Im}\,G^{j|j'}_{-\zeta\varepsilon_n^{j|j'}}(\omega|\omega'), \tag{142}$$

where

$$\varepsilon_n^{j|j'} = (-1)^n \zeta^{1+m^{j|j'}}. \tag{143}$$

Utilizing (91) we finally achieve the representation

$$\mathrm{Re}\, G^{j|j'}_{\varepsilon_n^{j|j'}}(\omega|\omega') = -\Big[1+\zeta 2 n_\zeta\big(\Delta^{j|j'}(\omega|\omega')\big)\Big]\,\mathrm{Re}\, G^{j|j'}_{-\varepsilon_n^{j|j'}}(\omega|\omega'), \tag{144}$$

$$\mathrm{Im}\, G^{j|j'}_{-\varepsilon_n^{j|j'}}(\omega|\omega') = -\Big[1+\zeta 2 n_\zeta\big(\Delta^{j|j'}(\omega|\omega')\big)\Big]\,\mathrm{Im}\, G^{j|j'}_{\varepsilon_n^{j|j'}}(\omega|\omega'). \tag{145}$$

These two equations express relations between certain linear combinations of the components of $G^{\alpha|\alpha'}$. Since the components of $G^{\alpha|\alpha'}$ can be understood in terms of higher order response and correlation functions [19], equations (144) and (145) constitute a multi-particle FDT. Both equations can be evaluated for $2^{2n}$ different realizations of the indices $(j|j')$. However, the underlying equation (133) is equivalent for $G^{j|j'}$ and for $G^{\bar{j}|\bar{j}'}$ as can be inferred from $m^{j|j'} = -m^{\bar{j}|\bar{j}'}$ and $\Delta^{j|j'}(\omega|\omega') = -\Delta^{\bar{j}|\bar{j}'}(\omega|\omega')$. Therefore only half of the $2^{2n}$ equations (144) are independent. The same applies to (145).

For bosons the function $n_{\zeta=+}\big(\Delta^{j|j'}(\omega|\omega')\big)$ diverges in the special case $\Delta^{j|j'}(\omega|\omega') \equiv 0$ (which occurs for all contour indices being $-$ or all being $+$), and one then should rather use (141) and (142) with $\cosh[\beta\Delta^{j|j'}(\omega|\omega')/2] = 1$ and $\sinh[\beta\Delta^{j|j'}(\omega|\omega')/2] = 0$ instead of (144) and (145).

The transformation of (134) to the Keldysh basis is completely analogous to that of (133). Defining for $\varepsilon = \pm 1$

$$\gamma_\varepsilon^{j'|j} = \sum_{\substack{\alpha',\alpha \\ (-1)^{\sum_k(\alpha'_k+\alpha_k)}=\varepsilon}} D^{j'|\alpha'}\gamma^{\alpha'|\alpha}(D^{-1})^{\alpha|j} \tag{146}$$

we end up with

$$\mathrm{Re}\,\gamma^{j'|j}_{\varepsilon_1^{j'|j}}(\omega'|\omega) = -\Big[1+\zeta 2 n_\zeta\big(\Delta^{j'|j}(\omega'|\omega)\big)\Big]\,\mathrm{Re}\,\gamma^{j'|j}_{-\varepsilon_1^{j'|j}}(\omega'|\omega), \tag{147}$$

$$\mathrm{Im}\,\gamma^{j'|j}_{-\varepsilon_1^{j'|j}}(\omega'|\omega) = -\Big[1+\zeta 2 n_\zeta\big(\Delta^{j'|j}(\omega'|\omega)\big)\Big]\,\mathrm{Im}\,\gamma^{j'|j}_{\varepsilon_1^{j'|j}}(\omega'|\omega), \tag{148}$$

where

$$\varepsilon_1^{j'|j} = -\zeta^{1+m^{j'|j}} \tag{149}$$

[cf. (143)]. Like in the case of Green functions, each of equations (147) and (148) contains only $2^{2n-1}$ independent relations.

Let us illustrate equations (144), (145) and (147), (148) by some examples. In the one-particle case, $n = 1$, we evaluate (144) and (145) for $(j|j') = (-|-)$ and $(j|j') = (-|+)$. Since $G^{-|-} = \frac{1}{2}(G^{1|2} + G^{2|1} + G^{2|2})$ and $G^{-|+} = \frac{1}{2}(G^{1|2} - G^{2|1} + G^{2|2})$, we have

$$G_+^{-|-} = \frac{1}{2}G^{2|2} = \frac{1}{2}G^{\mathrm{K}}, \tag{150}$$

$$G_-^{-|-} = \frac{1}{2}(G^{1|2} + G^{2|1}) = \frac{1}{2}(G^{\mathrm{Av}} + G^{\mathrm{Ret}}), \tag{151}$$

$$G_+^{-|+} = \frac{1}{2}G^{2|2} = \frac{1}{2}G^{\mathrm{K}}, \tag{152}$$

$$G_-^{-|+} = \frac{1}{2}(G^{1|2} - G^{2|1}) = \frac{1}{2}(G^{\mathrm{Av}} - G^{\mathrm{Ret}}). \tag{153}$$

Furthermore, we use

$$\Delta^{-|-}(\omega|\omega') = 0, \qquad \varepsilon_1^{-|-} = -\zeta, \tag{154}$$

$$\Delta^{-|+}(\omega|\omega') = \omega' - \mu, \qquad \varepsilon_1^{-|+} = -1, \tag{155}$$

and the representation of the one-particle Green function $G(\omega|\omega') = 2\pi\delta(\omega-\omega')G(\omega)$. Then equations (144) and (145) evaluated for $(j|j') = (-|-),(-|+)$ read

$$\mathrm{Re}\, G^{\mathrm{K}}(\omega) = 0, \tag{156}$$

$$\mathrm{Re}\left[G^{\mathrm{Av}}(\omega) - G^{\mathrm{Ret}}(\omega)\right] = -\left[1+\zeta 2n_\zeta(\omega-\mu)\right]\mathrm{Re}\, G^{\mathrm{K}}(\omega) = 0, \tag{157}$$

$$\mathrm{Im}\left[G^{\mathrm{Av}}(\omega) + G^{\mathrm{Ret}}(\omega)\right] = 0, \tag{158}$$

$$\mathrm{Im}\, G^{\mathrm{K}}(\omega) = -\left[1+\zeta 2n_\zeta(\omega-\mu)\right]\mathrm{Im}\left[G^{\mathrm{Av}}(\omega) - G^{\mathrm{Ret}}(\omega)\right]. \tag{159}$$

These formulae obviously reproduce (54) and (89) under the additional constraint $G_{q|q'}(\omega) = G_{q'|q}(\omega)$ which follows from the special one-particle property (109) and the assumption (117).

Evaluating (147) and (148) for the one-particle vertex (the self-energy), leads to a result similar to (156) – (159): one only needs to replace $G$ therein by the self-energy $\Sigma$.

For $n = 2$ the complete set of relations for the Green functions is obtained by evaluating (144) and (145) for eight independent choices for $(j_1 j_2|j_1' j_2')$ from 16 existing possibilities. Let us for example discuss the three particular combinations $(j_1 j_2|j_1' j_2') = (--|--),(-+|--),(--|++)$. Since

$$\Delta^{--|--}(\omega_1,\omega_2|\omega_1',\omega_2') = 0, \qquad \varepsilon_2^{--|--} = \zeta, \tag{160}$$

$$\Delta^{-+|--}(\omega_1,\omega_2|\omega_1',\omega_2') = -\omega_2 + \mu, \qquad \varepsilon_2^{-+|--} = +1, \tag{161}$$

$$\Delta^{--|++}(\omega_1,\omega_2|\omega_1',\omega_2') = \omega_1' + \omega_2' - 2\mu, \qquad \varepsilon_2^{--|++} = \zeta, \tag{162}$$

equations (144) and (145) read

$$\mathrm{Re}\, G_-^{--|--}(\omega_1,\omega_2|\omega_1',\omega_2') = 0, \tag{163}$$

$$\mathrm{Im}\, G_+^{--|--}(\omega_1,\omega_2|\omega_1',\omega_2') = 0, \tag{164}$$

$$\mathrm{Re}\, G_+^{-+|--}(\omega_1,\omega_2|\omega_1',\omega_2') = -\left[1+\zeta 2n_\zeta(-\omega_2+\mu)\right]\mathrm{Re}\, G_-^{-+|--}(\omega_1,\omega_2|\omega_1',\omega_2'), \tag{165}$$

$$\mathrm{Im}\, G_-^{-+|--}(\omega_1,\omega_2|\omega_1',\omega_2') = -\left[1+\zeta 2n_\zeta(-\omega_2+\mu)\right]\mathrm{Im}\, G_+^{-+|--}(\omega_1,\omega_2|\omega_1',\omega_2'), \tag{166}$$

$$\mathrm{Re}\, G_\zeta^{--|++}(\omega_1,\omega_2|\omega_1',\omega_2') = -\left[1+\zeta 2n_\zeta(\omega_1'+\omega_2'-2\mu)\right]\mathrm{Re}\, G_{-\zeta}^{--|++}(\omega_1,\omega_2|\omega_1',\omega_2'), \tag{167}$$

$$\mathrm{Im}\, G_{-\zeta}^{--|++}(\omega_1,\omega_2|\omega_1',\omega_2') = -\left[1+\zeta 2n_\zeta(\omega_1'+\omega_2'-2\mu)\right]\mathrm{Im}\, G_\zeta^{--|++}(\omega_1,\omega_2|\omega_1',\omega_2'). \tag{168}$$

The functions $G_\pm^{j_1 j_2|j_1' j_2'}$ appearing in these equations can be found by explicit evaluation of (136) with help of (29) – (31). This results in

$$G_+^{--|--} = \frac{1}{4}\left(G^{11|11}+G^{11|22}+G^{12|12}+G^{12|21}+G^{21|12}+G^{21|21}+G^{22|11}\right), \tag{169}$$

$$G_-^{--|--} = \frac{1}{4}\left(G^{11|12}+G^{11|21}+G^{12|11}+G^{21|11}+G^{22|21}+G^{22|12}+G^{21|22}+G^{12|22}\right), \tag{170}$$

$$G_+^{-+|--} = \frac{1}{4}\left(-G^{11|11}-G^{11|22}+G^{12|12}+G^{12|21}-G^{21|12}-G^{21|21}+G^{22|11}\right), \tag{171}$$

$$G_-^{-+|--} = \frac{1}{4}\left(-G^{11|12}-G^{11|21}+G^{12|11}-G^{21|11}+G^{22|21}+G^{22|12}-G^{21|22}+G^{12|22}\right), \tag{172}$$

$$G_{+}^{--|++} = \frac{1}{4}\big(G^{11|11} + G^{11|22} - G^{12|12} - G^{12|21} - G^{21|12} - G^{21|21} + G^{22|11}\big), \tag{173}$$

$$G_{-}^{--|++} = \frac{1}{4}\big(-G^{11|12} - G^{11|21} + G^{12|11} + G^{21|11} - G^{22|21} - G^{22|12} + G^{21|22} + G^{12|22}\big). \tag{174}$$

## 6. Conservation of the properties in approximations

In practice the Green and vertex functions can often be computed only in approximations. In this section, we address the question whether such approximations are consistent with the exact relations presented in this review. Since the answer depends on the details of the corresponding method, we have to restrict ourselves to specific approximation schemes. First we discuss the large class of diagrammatic approximations, and then we analyse approximations within the framework of the fRG.

### *6.1. Diagrammatic approximations*

Many of the approximations used to compute the Green or vertex functions are given by taking into account only a subset of all diagrams contributing to that function. This may be either a finite set like in perturbation theory or an infinite one like in the random phase approximation. We call this approach a diagrammatic approximation and assume that apart from choosing only a subset of diagrams no further approximation is done. Since all discussed relations are linear in the vertex functions it follows that if two distinct diagrammatic approximations satisfy a given relation each, so does their sum.

Consider a diagrammatic approximation to a multi-particle Green or vertex function. The condition for the approximation to fulfil the relation (45) or (46) under permutations of particles is that the set of diagrams taken into account is invariant under those permutations. For instance neither of the diagrams in figure 4 alone fulfils the relation (46). The approximation given by the sum of diagram (a) and (b) in figure 4 satisfies a part of (46), namely

$$\gamma^{Pj'|j}_{Pq'|q}(P\omega'|\omega) = \zeta^{P}\gamma^{j'|j}_{q'|q}(\omega'|\omega). \tag{175}$$

The same is true for the sum of (c) and (d). The sum of (a) and (c) satisfies

$$\gamma^{j'|Pj}_{q'|Pq}(\omega'|P\omega) = \zeta^{P}\gamma^{j'|j}_{q'|q}(\omega'|\omega), \tag{176}$$

so does the sum of (b) and (d). The sum of (a) and (d) satisfies

$$\gamma^{Pj'|Pj}_{Pq'|Pq}(P\omega'|P\omega) = \gamma^{j'|j}_{q'|q}(\omega'|\omega), \tag{177}$$

as does the sum of (b) and (c). Only the sum of all four diagrams fulfils the complete relation (46). In practice one will exploit the symmetry imposed by (46) to reduce the number of components which have to be evaluated directly. For instance, it would be sufficient to calculate one of the four diagrams in figure 4 and use the result to derive the other three diagrams via (46).

Since complex conjugation of a Green function interchanges creation and annihilation operators it reverses the direction of lines in diagrams. This results in the following criterion for a diagrammatic approximation to comply with equation (48) or (50) [or equivalently (52) or (53)]: the set of diagrams taken into account has to be invariant under reversion of the directed lines combined with the simultaneous exchange of the external indices $j$ with $j'$, $q$ with $q'$, and $\omega$ with $\omega'$. For example, reversing the direction of all lines in figure 4 (a) and interchanging 1 with $1'$ and 2 with $2'$ reproduces the same diagram. Hence, an approximation

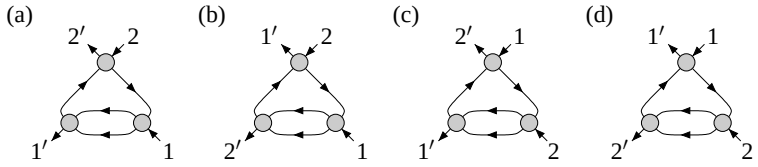


**Figure 4.** Examples of diagrams contributing to the two-particle vertex function $\gamma_{1'2'|12}$. The external indices represent contour index, state and frequency, e.g. $1 = (j_1, q_1, \omega_1)$.

to the two-particle vertex function consisting only of this single diagram complies with (50). The same holds for figure 4 (d). The diagram in figure 4 (b) is mapped onto that of figure 4 (c) by complex conjugation and vice versa. The approximation given by their sum fulfils (50). Similarly to the rules for permutation of particles, one will use (48) or (50) in practice in order to reduce the number of components one has to evaluate directly.

The theorem of causality for the vertex function has been proven in section 4.3 for each single diagram; the theorem of analyticity is a direct consequence of it. Therefore, both theorems hold in any diagrammatic approximation to the vertex functions. Given the causal features of the noninteracting single-particle Green function, the theorem of causality for the interacting multi-particle Green function can also be proven to hold for any single diagram. The proof is analogous to the one for the diagrams of vertex functions given in section 4.3. That's why the theorems of causality and analyticity for the Green functions hold in any diagrammatic approximation as well.

The proof of the KMS condition (113) for the vertex functions has been performed diagram per diagram. The same applies to the special form (132) which brings about (147) and (148). Hence (113) and (147), (148) hold in any diagrammatic approximation to the vertex functions. Again, an analogous proof for the diagrams of the interacting Green function can be formulated, showing that equations (108), (144), and (145) hold in any diagrammatic approximation to the Green functions.

### *6.2. Functional renormalization group*

While diagrammatic approximations automatically preserve causality and the KMS conditions, these features can be much more difficult to maintain in other approximation schemes. We briefly sketch complications for the fRG approach which is based on introducing a flow parameter $\Lambda$ into the free single-particle Green functions; typically this is done in such a way that degrees of freedom at energies below $\Lambda$ are suppressed in order to regularize low energy divergencies which may arise in perturbation theory. The vertex functions, expressed as functionals of the free single-particle Green functions, depend on $\Lambda$ and can be computed as solutions of a coupled set of flow equations [22, 23, 24].

Let us consider the flow of the one-particle irreducible vertex functions $\gamma_{n;\Lambda}$ governed by the hierarchy of the fRG equations

$$\frac{\mathrm{d}}{\mathrm{d}\Lambda}\gamma_{1;\Lambda}^{\nu'|\nu} = \zeta\,\gamma_{2;\Lambda}^{\nu'\lambda'|\nu\lambda} S_{\Lambda;\lambda|\lambda'}, \tag{178}$$

$$\begin{aligned}\frac{\mathrm{d}}{\mathrm{d}\Lambda}\gamma_{2;\Lambda}^{\nu_1'\nu_2'|\nu_1\nu_2} &= \zeta\,\gamma_{3;\Lambda}^{\nu_1'\nu_2'\lambda'|\nu_1\nu_2\lambda} S_{\Lambda;\lambda|\lambda'} + \gamma_{2;\Lambda}^{\nu_1'\nu_2'|\lambda_1\lambda_2} G_{\Lambda;\lambda_1|\lambda_1'} S_{\Lambda;\lambda_2|\lambda_2'} \gamma_{2;\Lambda}^{\lambda_1'\lambda_2'|\nu_1\nu_2} \\ &\quad + \Big\{ G_{\Lambda;\lambda_1|\lambda_2'} S_{\Lambda;\lambda_2|\lambda_1'} \Big[ \zeta\,\gamma_{2;\Lambda}^{\nu_1'\lambda_1'|\nu_1\lambda_1} \gamma_{2;\Lambda}^{\lambda_2'\nu_2'|\lambda_2\nu_2} + \gamma_{2;\Lambda}^{\nu_1'\lambda_1'|\lambda_1\nu_2} \gamma_{2;\Lambda}^{\lambda_2'\nu_2'|\nu_1\lambda_2} \Big] + (G_\Lambda \leftrightarrow S_\Lambda) \Big\},\end{aligned} \tag{179}$$

$$\ldots, \tag{180}$$

where $\gamma_{1;\Lambda} \equiv \Sigma_\Lambda$, and the multi-indices $\nu$ and $\lambda$ comprise frequency (time) argument as well as the state and the Keldysh indices; a summation convention applies to multi-indices appearing twice in a product. The dots in (180) represent the flow equations for $\gamma_{3;\Lambda}, \gamma_{4;\Lambda}, \ldots$. The notation $S_\Lambda$ stands for the so-called single scale propagator which is defined by

$$S_{\Lambda;\lambda|\lambda'} = -G_{\Lambda;\lambda|\nu} \left( \frac{\mathrm{d}(G_\Lambda^{(0)})^{-1}}{\mathrm{d}\Lambda} \right)^{\nu|\nu'} G_{\Lambda;\nu'|\lambda'}. \tag{181}$$

The equations (178) – (180) can be systematically obtained from the vertex generating functional explicitly depending of the flow parameter $\Lambda$ [24, 10]. An equivalent derivation is based on a purely diagrammatic approach [11] in which $\Lambda$ is explicitly introduced into the free propagators $G^{(0)}$.

Since the flow of $\gamma_{n;\Lambda}$ is determined by $\gamma_{1;\Lambda}, \ldots, \gamma_{n;\Lambda}$ and $\gamma_{n+1;\Lambda}$, the exact flow equations (178–180) form an infinite coupled hierarchy. The final solution of the full hierarchy is exact and therefore satisfies all relations discussed in the previous sections. However, in nontrivial practical problems one cannot solve the full hierarchy but has to resort to approximations. Typically one truncates the hierarchy of flow equations which means setting $\mathrm{d}\gamma_{n;\Lambda}/\mathrm{d}\Lambda = 0$ for some $n$, such that the flow equations for $\gamma_{1;\Lambda}, \ldots, \gamma_{n-1;\Lambda}$ form a finite closed set. Then it is no longer guaranteed that the final solution of the truncated flow equations satisfies the exact relations in question. It turns out that the choice of the flow parameter has a decisive influence on their conservation. While arbitrary choices of the flow parameter do not affect the properties under permutation of particles and complex conjugation, special care is required in order to maintain the theorem of causality and the KMS conditions.

Assuming that the only approximation done to the flow equation is a truncation of the hierarchy we find the following sufficient conditions for the construction of conserving flow parameters. (1) If the free propagator $G_\Lambda^{(0)}$ furnished with the flow parameter $\Lambda$ satisfies the theorem of causality, then the vertex functions resulting from a truncated set of flow equations fulfil the theorem of causality throughout the flow and in the final solution. (2) If $G_\Lambda^{(0)}$ satisfies the fluctuation dissipation theorem (89) (with the factor $\left[1 + \zeta 2 n_\zeta(\omega - \mu)\right]$ not depending on $\Lambda$) then the vertex functions resulting from a truncated set of flow equations fulfil the KMS conditions throughout the flow and in the final solution.

For the proof of these rules we recall that the theorem of causality and the KMS conditions for the vertex functions have been derived in sections 4.3 and 5.4 for each single contributing diagram on the basis of the corresponding property of the free propagator $G^{(0)}$. In reference [11] the flow equations for the vertex functions have been derived from the individual diagrams contributing to $\mathrm{d}\gamma_{n;\Lambda}/\mathrm{d}\Lambda$, which contain lines $G_\Lambda^{(0)}$ and one line $\mathrm{d}G_\Lambda^{(0)}/\mathrm{d}\Lambda$. If $G_\Lambda^{(0)}$ and $\mathrm{d}G_\Lambda^{(0)}/\mathrm{d}\Lambda$ satisfy the theorem of causality, then the same arguments as applied in section 4.3 can be used to prove the theorem of causality for each single diagram contributing to $\mathrm{d}\gamma_{n;\Lambda}/\mathrm{d}\Lambda$. Truncating flow equations means taking into account only a subset of these diagrams and it thus has no influence on the conservation of causality during the flow. Note that the theorem of causality for $\mathrm{d}G_\Lambda^{(0)}/\mathrm{d}\Lambda$ follows from that of $G_\Lambda^{(0)}$ since the derivative is a linear operation. Concerning the KMS conditions we can argue analogously.

As examples for these considerations we discuss different flow parameters used in the literature and propose also a new one. In reference [10] the flow parameter is introduced into the free Green function by setting

$$G_\Lambda^{(0)}(\omega) = \Theta(|\omega| - \Lambda) G^{(0)}(\omega). \tag{182}$$

Since the step function $\Theta(z)$ has a branch-cut along the imaginary axis of $z$, the analytic properties of $G_\Lambda^{(0)}(\omega)$ are in contradiction to the theorem of causality: $G_\Lambda^{(0)}(\omega)$ being

nonanalytic in the upper half plane implies that $G_\Lambda^{(0)\,\mathrm{Ret}}(t|t') = G_\Lambda^{(0)\,2|1}(t|t')$ does not vanish for $t' > t$. As a consequence the vertex functions constructed from diagrams with lines given by $G_\Lambda^{(0)}$ instead of $G^{(0)}$ do not exhibit the correct causal features. When the exact RG flow stops at $\Lambda = 0$, causality is restored due to $G_{\Lambda=0}^{(0)} = G^{(0)}$. However, for nontrivial models the flow equations for the vertex functions can be solved only approximately. Restoring causality for approximate solutions of the flow equations was encountered as a major difficulty in reference [10].

This problem can be solved if one chooses a flow parameter such that $G_\Lambda^{(0)}(\omega)$ has the same analytic features as $G^{(0)}(\omega)$. Then the causal features of the vertex functions are preserved during all the RG flow, even for truncated flow equations. An example of such a flow parameter is the imaginary frequency cut-off proposed in reference [11] which manipulates the particle distribution functions of the reservoirs by

$$n_\zeta(\omega) = \frac{1}{\mathrm{e}^{\beta\omega} - \zeta} = T\sum_{\omega_n} \frac{\mathrm{e}^{\mathrm{i}\omega_n 0^+}}{\mathrm{i}\omega_n - \omega} \qquad \to \qquad n_\zeta^\Lambda(\omega) = T\sum_{\omega_n} \frac{\Theta(|\omega_n| - \Lambda)\mathrm{e}^{\mathrm{i}\omega_n 0^+}}{\mathrm{i}\omega_n - \omega}, \quad (183)$$

where $\omega_n = 2n\pi T$ or $\omega_n = (2n+1)\pi T$ denote the Matsubara frequencies for bosons or fermions, respectively. This cut-off affects only the Keldysh component of the free single-particle Green function, but not the retarded or advanced ones which contain only dynamical but no statistical information, $G_\Lambda^{(0)\mathrm{Ret/Av}}(\omega) = G^{(0)\mathrm{Ret/Av}}(\omega)$. Hence, the causal properties of free single-particle Green function are unchanged and causal features of the vertex functions are conserved. However, since the $\Lambda$-dependent distribution function in (183) is not the thermal one, the single-particle Green function $G_\Lambda^{(0)}$ does not fulfil the fluctuation dissipation theorem for $\Lambda \neq 0$. As a consequence the KMS conditions for the vertex functions are not satisfied until the exact flow terminates at $\Lambda = 0$. Solvable approximations to the flow equations will in general not restore the KMS-conditions even at $\Lambda = 0$. (The simple static approximation used in reference [11] yet satisfies the KMS-conditions in a trivial way.)

Examples of flow parameters which violate neither causality nor the KMS conditions are given by the momentum cut-off and by the hybridization of the system and reservoirs.

The momentum cut-off is introduced for extended systems by defining

$$G_{k;\Lambda}^{(0)\mathrm{Ret/Av/K}}(\omega) = \Theta(|\varepsilon_k| - \Lambda) G_k^{(0)\mathrm{Ret/Av/K}}(\omega), \quad (184)$$

where the wave number $k$ labels a single-particle eigenstate with eigenenergy $\varepsilon_k$. Obviously, this cut-off does not affect the frequency dependence of $G^{(0)}$; hence, it preserves causality and the KMS conditions.

We propose to use hybridization as a flow parameter which is useful for local systems coupled to external reservoirs. After integrating out reservoir states, the Green function of a local system acquires a reservoir broadening $\Gamma$. For example, the reservoir-dressed Green function of the SIAM defined in (118) reads

$$G_\sigma^{(0)\mathrm{Ret}}(\omega) = \frac{1}{\omega - (\varepsilon_0 + \sigma B) + \frac{\mathrm{i}}{2}\Gamma}, \quad (185)$$

where $\Gamma = 2\pi\sum_p \delta(\mu - \varepsilon_p)|V_p|^2$. The idea of the hybridization flow parameter consists in introducing an additional – fictitious – reservoir, which is assumed to be in thermodynamical equilibrium with the physical one, i.e. is characterized by the same temperature $T$ and chemical potential $\mu$. The flow parameter $\Lambda$ is then associated with an additional broadening due to a coupling to the fictitious reservoir, so that

$$G_{\sigma;\Lambda}^{(0)\mathrm{Ret}}(\omega) = \frac{1}{\omega - (\varepsilon_0 + \sigma B) + \frac{\mathrm{i}}{2}(\Gamma + \Lambda)}, \quad (186)$$

$$G^{(0)\mathrm{Av}}_{\sigma;\Lambda}(\omega) = G^{(0)\mathrm{Ret}}_{\sigma;\Lambda}(\omega)^*, \tag{187}$$

$$G^{(0)\mathrm{K}}_{\sigma;\Lambda}(\omega) = \left[1+\zeta 2n_\zeta(\omega-\mu)\right]\left[G^{(0)\mathrm{Ret}}_{\sigma;\Lambda}(\omega) - G^{(0)\mathrm{Av}}_{\sigma;\Lambda}(\omega)\right]. \tag{188}$$

In the beginning of the flow at $\Lambda = \infty$, the free propagator is suppressed and the vertex functions are identical to their bare values (except for the self-energy which acquires a final contribution from the Hartree-Fock diagram, $\Sigma^{\mathrm{Ret}}_{q'|q;\Lambda=\infty} = \frac{1}{2}\sum_p \bar{v}_{q'p|qp}$). In the end of the flow at $\Lambda = 0$ the fictitious reservoir is decoupled, and we restore the original system. Since $G^{(0)}_\Lambda$ in (186–188) satisfies the theorem of causality and the fluctuation dissipation theorem, causality and the KMS conditions of the vertex functions are preserved during the flow, even when the flow equations are truncated. A detailed study of the SIAM on basis of the hybridization flow is presented in [25], where it is also generalized to nonequilibrium situations.

## 7. Conclusion

Currently the interest in nonequilibrium dynamics and in the crossover between equilibrium and nonequilibrium properties is enormously increasing in the field of condensed matter physics. Keldysh formalism provides the possibility to treat equilibrium and nonequilibrium quantum systems on equal footing. Numerous equilibrium techniques based on Green or vertex functions benefit a lot from adaptation to Keldysh formalism. For its correct implementation the knowledge of real time (frequency) features of the multi-component Green and vertex functions appears to be mandatory. The present review lists general properties of these functions in equilibrium and nonequilibrium stationary state.

The relations for the Green functions have been derived directly from their definition as expectation value of contour ordered operator product. The corresponding equations for the vertex functions have been obtained from the rules for the evaluation of irreducible diagrams.

We have surveyed the relations for permutations of particles (45, 46) and complex conjugation (48, 50) and cast them into the form convenient in practical use. In section 4.3 we have formulated the causality theorem and identified the components of the Green and vertex functions which are analytic in a certain half plane of the corresponding frequency arguments. These analytic features should be maintained throughout any approximation to the Green and vertex functions, otherwise the fundamental property of causality is violated.

A major part of the review has been devoted to the study of the KMS conditions which hold in equilibrium. We have worked out the constraints which equilibrium imposes on the multi-particle functions. They are given by the relationships (108, 113) to the multi-particle functions of the time reversed system. The connection to the FDT for single-particle functions has been extensively discussed. In particular we have determined the reason for its special form (89) for $n = 1$: it follows from the peculiar single-particle property (43). Furthermore, we identified an important class of systems with special behaviour (117) under time reversal which allow for a simplified formulation (144, 145, 147, 148) of the multi-particle FDT.

Finally we discussed how the properties in question relate to diagrammatic approximations and to approximations within the fRG. For diagrammatic approximations we found that the set of diagrams taken into account should be invariant under permutations within the incoming and within the outgoing external indices and invariant under reversal of the directed lines. Then the relations for permutation of particles and complex conjugation hold and reduce considerably the number of independent components which simplifies a treatment of a problem. Causal features and KMS conditions are preserved automatically in any diagrammatic approximation. However, approximations to the flow equations of the fRG often destroy causality and the KMS conditions. These properties can be preserved when

the flow parameter is appropriately chosen in such a way that it respects the corresponding properties of the noninteracting single-particle Green function.

## Acknowledgments

SGJ. thanks F Reininghaus, U Heinz and E Wang for helpful discussions. This work was supported by the DFG-Forschergruppe 723.

## References

[1] Negele J W and Orland H 1988, *Quantum Many-Particle Systems* (Reading, MA: Addison-Wesley)
[2] Salmhofer M 1998, *Renormalization: An Introduction* (Heidelberg: Springer)
[3] Bickers N E and Scalapino D J 1989 Conserving approximations for strongly fluctuating electron systems. I. Formalism and calculational approach *Ann. Phys., NY* **193** 206–51
[4] de Dominicis C and Martin P C 1964 Stationary entropy principle and renormalization in normal and superfluid systems: I. Algebraic formulation *J. Math. Phys.* **5** 14–30
[5] Bickers N E 1991 Parquet equations for numerical self-consistent-field theory *Int. J. Mod. Phys.* B **5** 253–70
[6] Beach K S D, Gooding R J and Marsiglio F 2000 Reliable Padé analytical continuation method based on a high-accuracy symbolic computation algorithm *Phys. Rev.* B **61** 5147–57
[7] Rammer J and Smith H 1986 Quantum field-theoretical methods in transport theory of metals *Rev. Mod. Phys.* **58** 323-59
[8] Haug H and Jauho A-P 1996 *Quantum Kinetics in Transport and Optics of Semiconductors* (Berlin: Springer)
[9] Lifshitz E M and Pitaevskii L P 1981 *Physical Kinetics* (New York: Pergamon Press)
[10] Gezzi R, Pruschke T and Meden V 2007 Functional renormalization group for nonequilibrium quantum many-body problems *Phys. Rev.* B **75** 045324
[11] Jakobs S G, Meden V and Schoeller H 2007 Nonequilibrium functional renormalization group for interacting quantum systems *Phys. Rev. Lett.* **99** 150603
[12] Chou K-C, Su Z-B, Hao B-L and Yu L 1985 Equilibrium and nonequilibrium formalisms made unified *Phys. Rep.* **118** 1–131
[13] Wang E and Heinz U 2002 Generalized fluctuation-dissipation theorem for nonlinear response functions *Phys. Rev.* D **66** 025008
[14] Kubo R 1957 Statistical-mechanical theory of irreversible processes: I. General theory and simple applications to magnetic and conduction problems *J. Phys. Soc. Japan* **12** 570–86
Kubo R 1966 The fluctuation-dissipation theorem *Rep. Prog. Phys.* **29** 255–84
[15] Martin P C and Schwinger J 1959 Theory of many-particle systems: I *Phys. Rev.* **115** 1342–73
[16] Anderson P W 1961 Localized magnetic states in metals *Phys. Rev.* **124** 41–53
[17] Danielewicz P 1984 Quantum theory of nonequilibrium processes I *Ann. Phys. (NY)* **152** 239–304
[18] Keldysh L V 1964 *Zh. Eksp. Teor. Fiz.* **47** 1515–27 [Diagram technique for nonequilibrium processes *Sov. Phys. JETP* **20** 1018–26 (1965)]
[19] Hao B-L 1981 Closed time path Green's functions and nonlinear response theory *Physica* A **109** 221–36
[20] Doyon B and Andrei N 2006 Universal aspects of nonequilibrium currents in a quantum dot *Phys. Rev.* B **73** 245326
[21] Messiah A 1962 *Quantum Mechanics* vol 2 (Amsterdam: North Holland Publishing Company)
[22] Wetterich C 1993 Exact evolution equation for the effective potential *Phys. Lett.* B **301** 90–94
[23] Morris T R 1994 The exact renormalization group and approximate solutions *Int. J. Mod. Phys.* A **9** 2411–2449
[24] Salmhofer M and Honerkamp C 2001 Fermionic renormalization group flows *Prog. Theor. Phys.* **105** 1–35
[25] Jakobs S G, Pletyukhov M and Schoeller H 2009 Nonequilibrium functional RG with frequency dependent vertex function: a study of the single impurity Anderson model *arXiv:0911.5502*